Instabilities in MHD accretion disks, accretion and outflows from magnetized stars

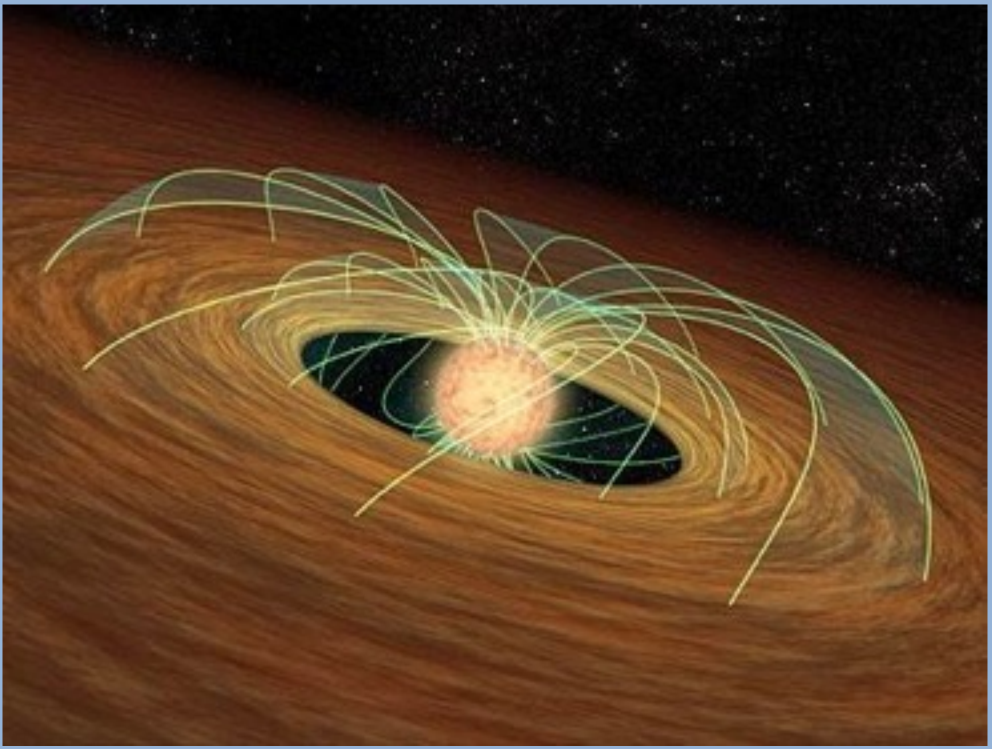

Richard Lovelace, Cornell University
Marina Romanova, Cornell University

25 August 2015

Plasma Astrophysics Group at Cornell

Richard Lovelace, Marina Romanova, graduate students: Sergei Dyda, Patrick Lii, Megan Comins; undergraduate student: Loren Malitsky

Different Stars Have Accretion Disks

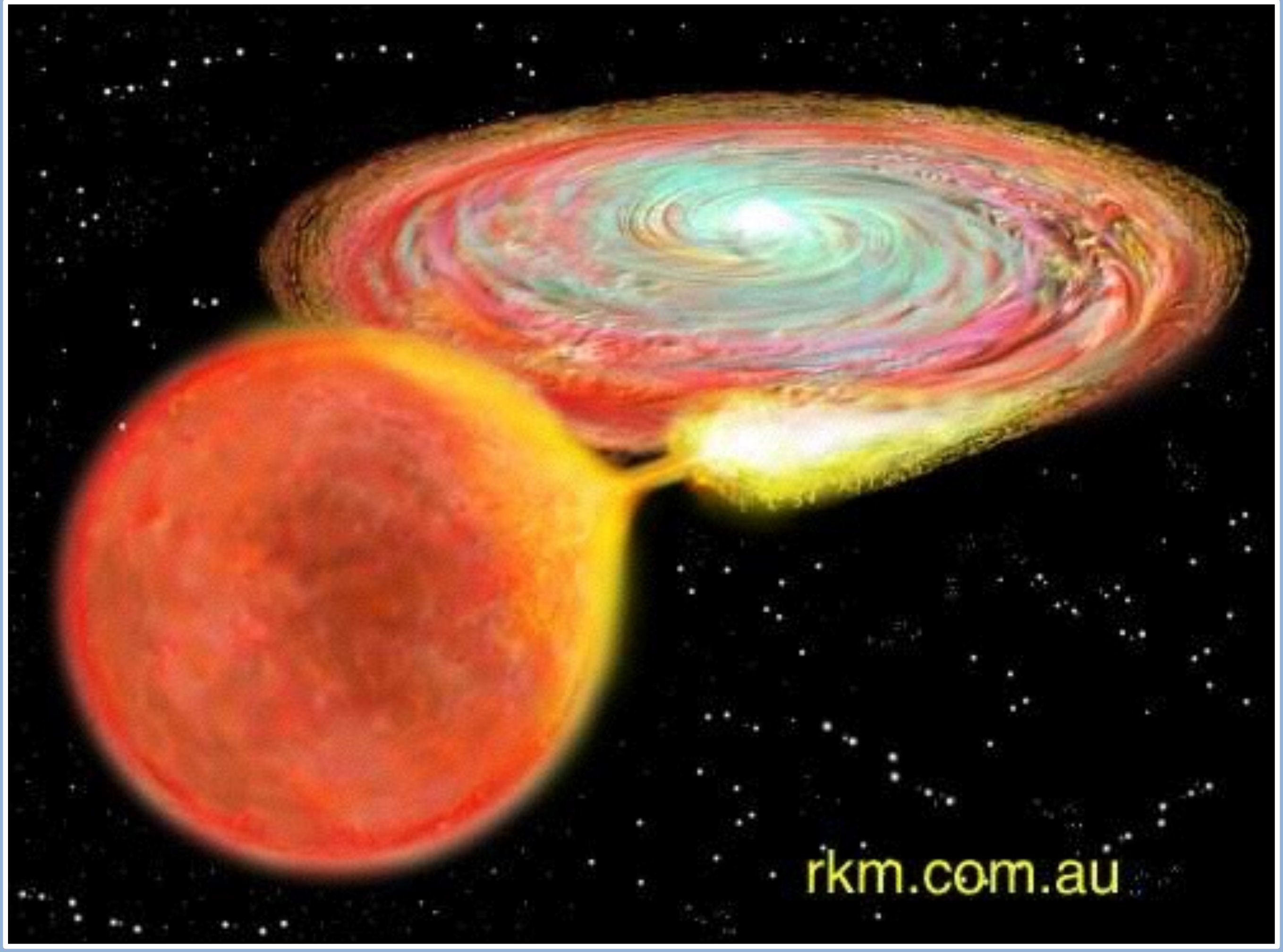

- The physics of accretion disks is not well known
- Turbulence, dynamo, Rossby waves ?

Many Stars Have Strong Magnetic Fields

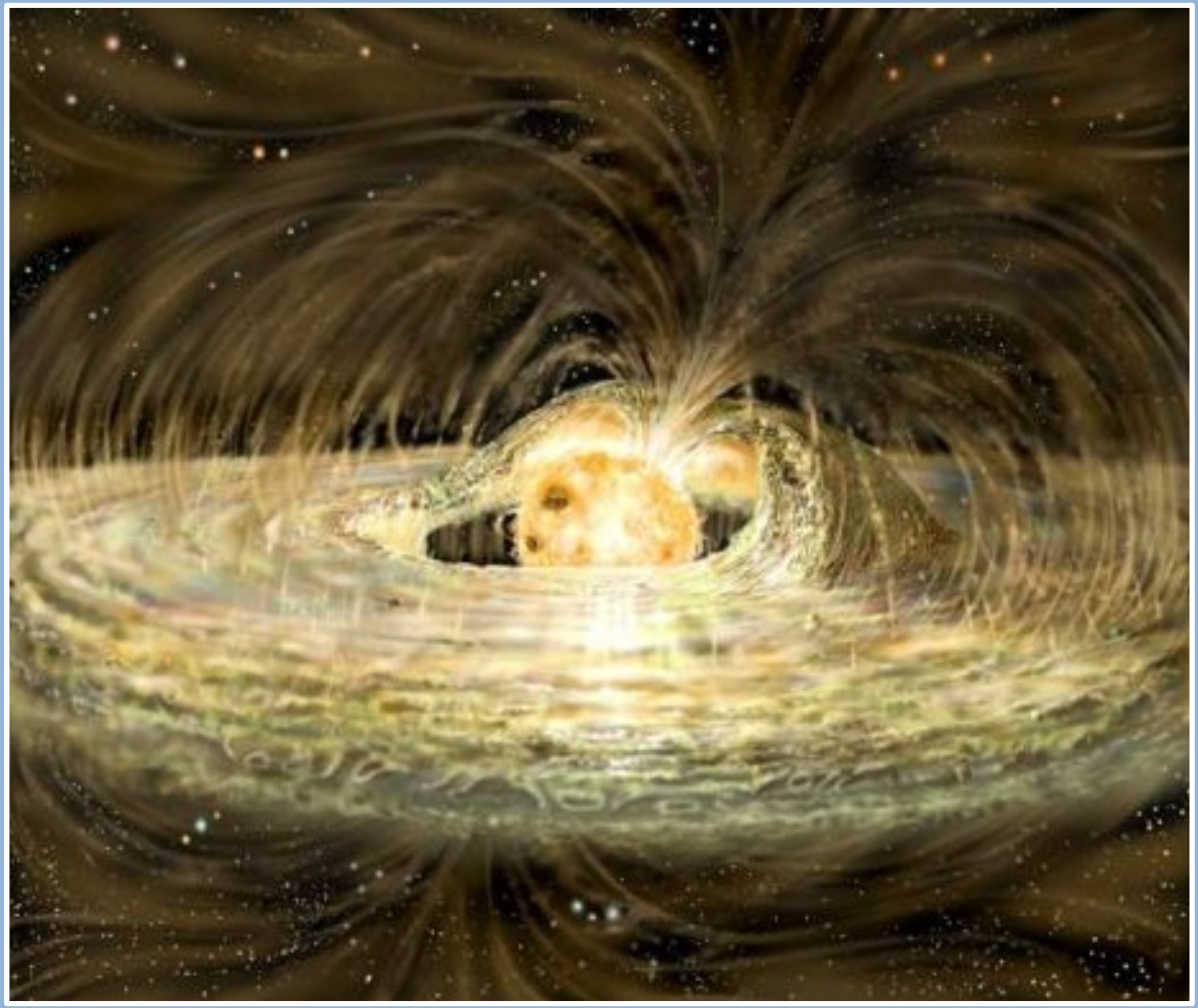

- For example, young Solar-type stars :1-5 kG field
- Accretion disk is disrupted by the stellar field

Jets and are Launched from Different Stars

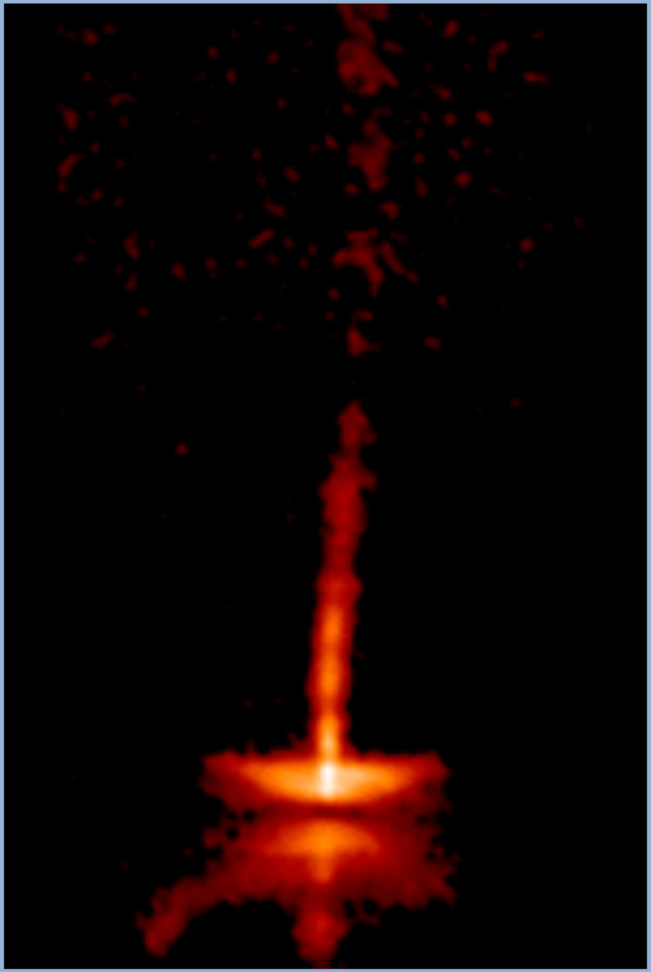

XZ Tau

HH 47

- An example of jest from young stars
- Launching and collimation are still open questions
- The magnetic mechanism is a possibility

Many Open Questions in Astrophysics

I. Physics of accretion disks, instabilities
II. Plasma Flow Around Magnetized Stars
III. Launching of Outflows and Jets

I. Instabilities in Accretion Disks

- Rossby Waves
- Dynamo
- Magneto-rotational Instability (MRI)
- Tearing Mode Instability
- Magnetic Interchange Instability

Paper with Norman Rostoker

Stability of annular equilibrium of energetic large orbit ion beam

H. Vernon Wong, H. L. Berk, R. V. Lovelace,[a] and N. Rostoker[b]
Institute for Fusion Studies, The University of Texas at Austin, Austin, Texas 78712

(Received 4 March 1991; accepted 1 July 1991)

The low-frequency stability of a long thin annular layer of energetic ions in a background plasma with finite axial and zero azimuthal magnetic field is studied analytically. It is found that although the equilibrium is susceptible to the kink instability, low mode number perturbations can be stabilized in the limit of $N_i/N_b \to 0$ when the current layer is close to the maximum field-reversal parameter. A brief discussion of the tearing mode stability criteria of such strong current layers with respect to the placement of conducting walls is also presented.

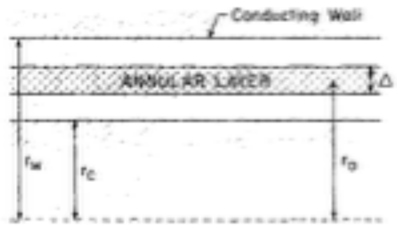

(a)

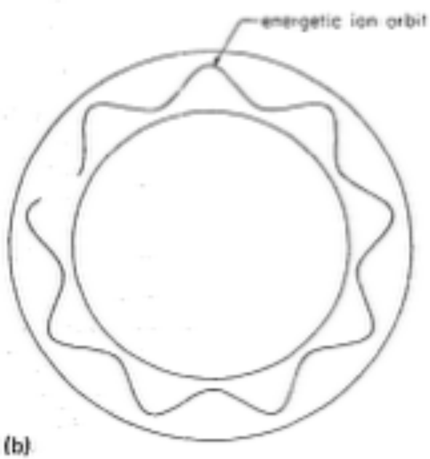

(b)

Rossby Waves in Accretion Disks

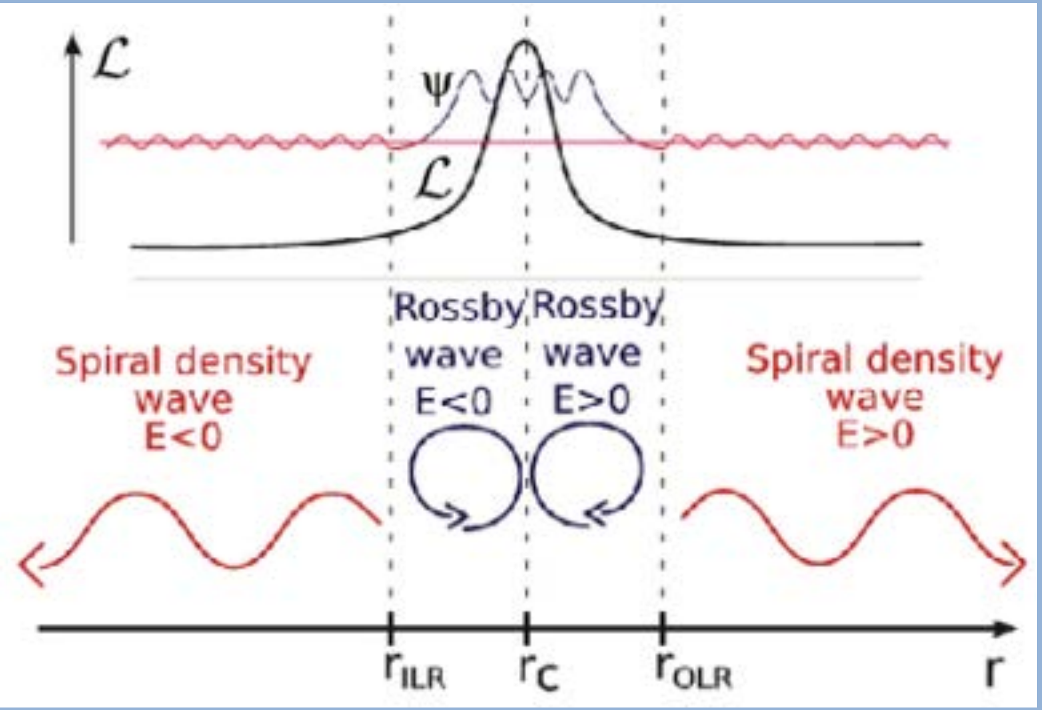

$$\mathcal{L}(r) = \frac{\Sigma\, S^{2/\gamma}}{2(\nabla \times \mathbf{u}) \cdot \hat{\mathbf{z}}}\,, \qquad (1)$$

at some radius r_0, where Σ is the surface mass density of the disc, $\Omega(r) \approx (GM_*/r^3)^{1/2}$ is the angular velocity of the flow (with M_* the mass of the central star), $\mathbf{u} \approx r\Omega(r)\hat{\phi}$ is the flow velocity of the disc, S is the specific entropy of the gas, and γ is the specific heat ratio. Note that $\mathcal{L}$ is related to the inverse of the *vortensity* which is defined as $(\nabla \times \mathbf{u})_z/\Sigma$. A sketch of a bump in $\mathcal{L}(r)$ is shown in Figure 1.

Lovelace & Hohlfeld 1978, Lovelace et al. 1999, Lovelace 2014

Effective Potential

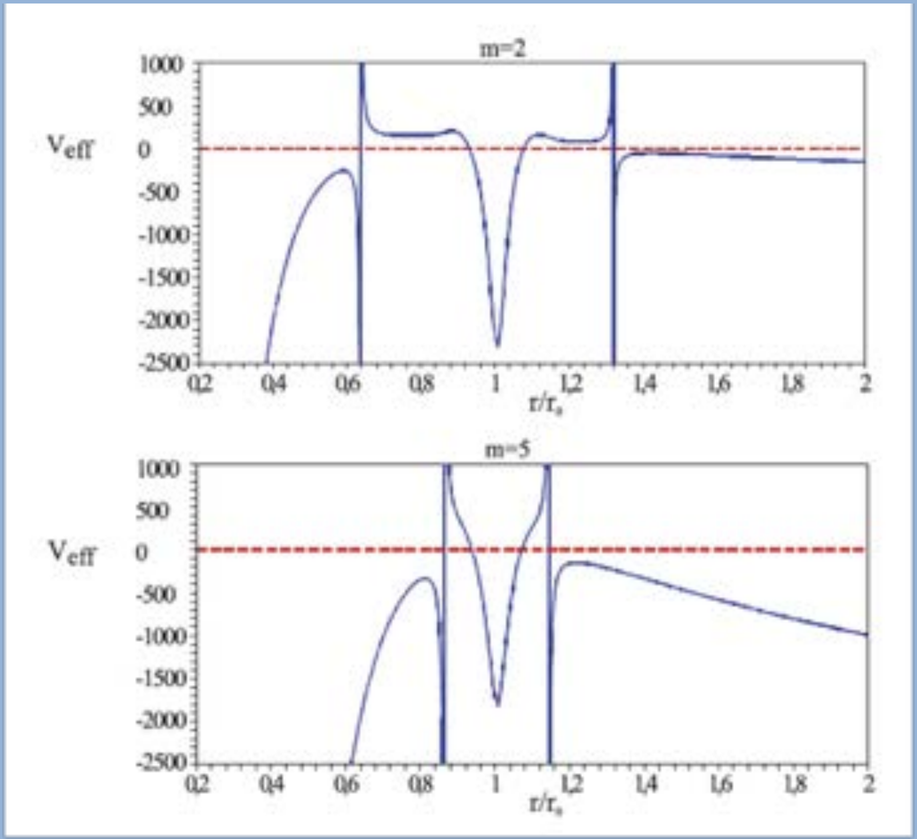

m=2

m=5

Lovelace 2014

Figure 2: Effective potential for a Gaussian surface density bump of peak amplitude $\Delta\Sigma/\Sigma = 0.2$ and width $\Delta r/r = 0.05$ for $m = 2$ (upper panel) and $m = 5$ (lower panel) adapted from [5]. Waves can propagate only in the regions where $V_{\text{eff}}(r) < 0$. The large positive values of V_{eff} occur at the inner and outer Lindblad resonance radii.

2D Simulations of Rossby Vortices

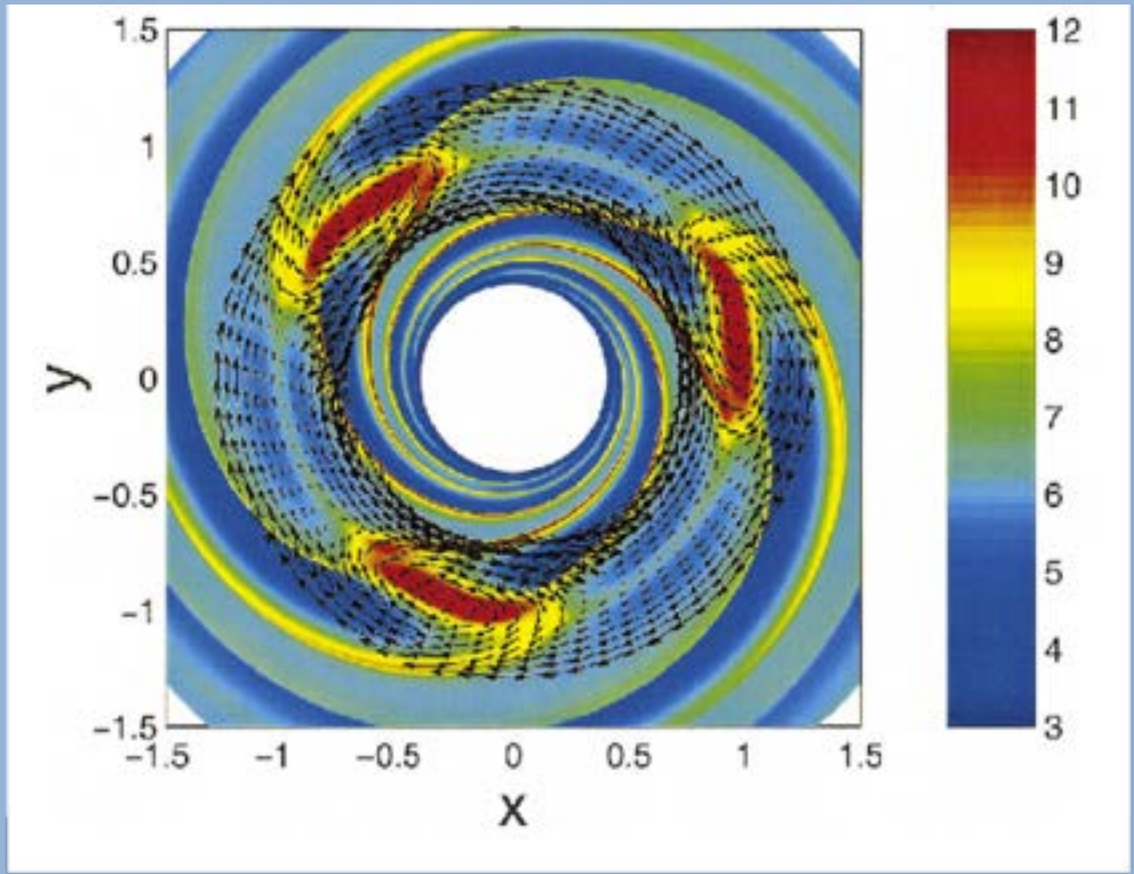

Lii et al. 2000

Figure 3: 2D hydrodynamic simulations of Rossby vortices in a disk adapted from [14] for $m = 3$. Pressure is color-coded (in units of $10^{-3}p_0$). Arrows indicate the flow pattern near r_0 in a comoving frame moving with velocity $u_\phi(r_0)$. The vortices are *anticyclonic*, enclosing high-pressure regions. Large-scale spirals are produced as well, in connection with the vortices.

Trapping of Dust by Rossby Vortices

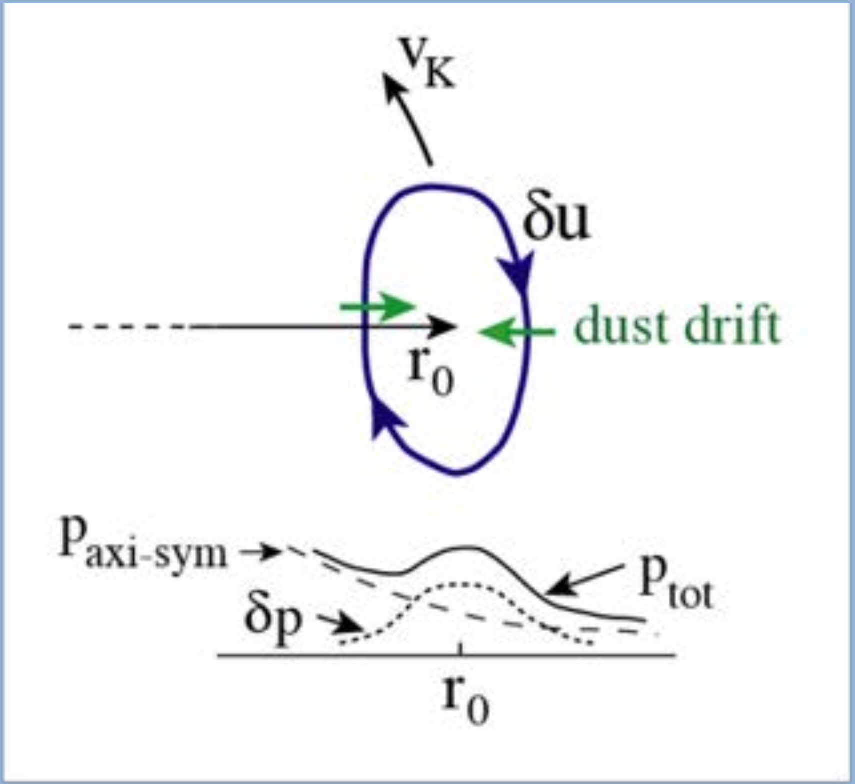

Lovelace 2014

Figure 4: Sketch of an anticyclonic vortex centered at radius r_0 in a Keplerian disc at some instant of time. The velocity perturbation of the vortex is $\delta\mathbf{u}$. The lower part of the figure sketches the radial pressure variation through the vortex center.

ALMA Observations of Protoplanetary Disks

From van der Marel et al., Science 340 p. 1199, 2013

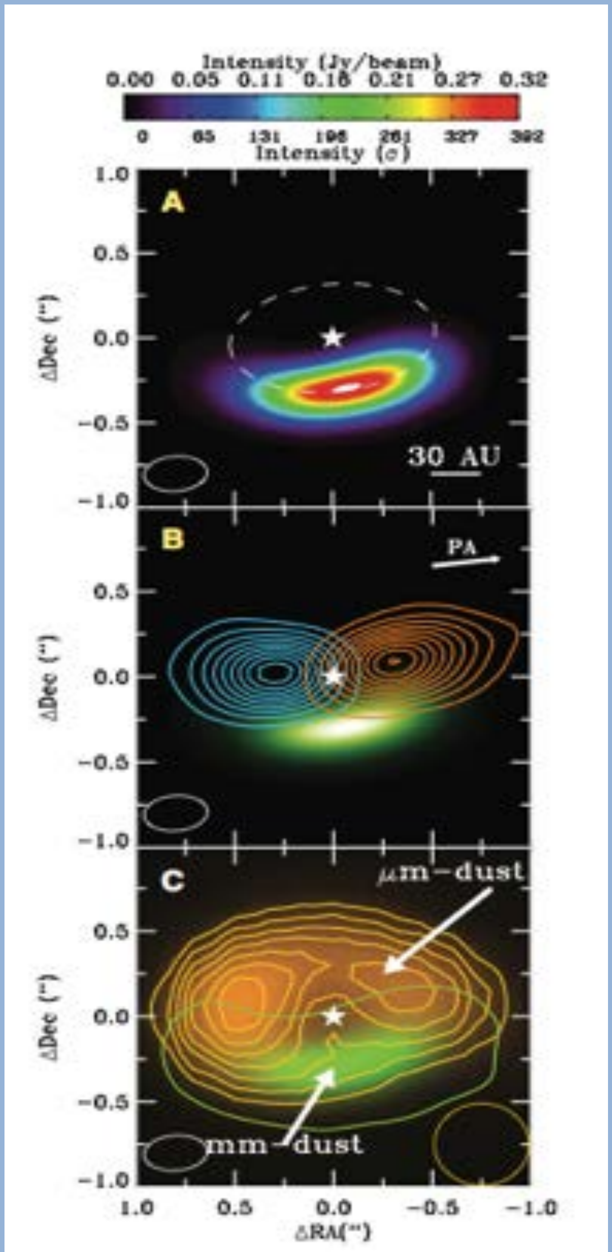

Magnetic Field Generation in Disc Dynamos

Axisymmetry $\Rightarrow \boldsymbol{B} = B\hat{\boldsymbol{\varphi}} + \boldsymbol{\nabla}\mathscr{A}\times\hat{\boldsymbol{\varphi}}/\varpi$, so B is the toroidal field strength and $\mathscr{A}$ is the flux function; both are functions of (ϖ, z) only, where ϖ is cylindrical radius. Expanding into components

$$
\begin{aligned}
\boldsymbol{B} &= B\hat{\boldsymbol{\varphi}} - \frac{\hat{\boldsymbol{\varpi}}}{\varpi}\frac{\partial\mathscr{A}}{\partial z} + \frac{\hat{\boldsymbol{z}}}{\varpi}\frac{\partial\mathscr{A}}{\partial\varpi} \\
\boldsymbol{\nabla}\times\boldsymbol{B} &= -\frac{\hat{\boldsymbol{\varphi}}}{\varpi}\left[\varpi\frac{\partial}{\partial\varpi}\left(\frac{1}{\varpi}\frac{\partial\mathscr{A}}{\partial\varpi}\right) + \frac{\partial^2\mathscr{A}}{\partial z^2}\right] - \hat{\boldsymbol{\varpi}}\frac{\partial B}{\partial z} + \frac{\hat{\boldsymbol{z}}}{\varpi}\frac{\partial(B\varpi)}{\partial\varpi}\,. \qquad (1)
\end{aligned}
$$

With a general velocity field $\boldsymbol{v} = \hat{\boldsymbol{\varphi}}\Omega\varpi + \hat{\boldsymbol{\varpi}}v_\varpi + \hat{\boldsymbol{z}}v_z$ we get

$$
\begin{aligned}
\boldsymbol{v}\times\boldsymbol{B} &= -\frac{\hat{\boldsymbol{\varphi}}}{\varpi}\left(v_\varpi\frac{\partial\mathscr{A}}{\partial\varpi} + v_z\frac{\partial\mathscr{A}}{\partial z}\right) + \hat{\boldsymbol{\varpi}}\left(\Omega\frac{\partial\mathscr{A}}{\partial\varpi} - v_z B\right) + \hat{\boldsymbol{z}}\left(v_\varpi B + \Omega\frac{\partial\mathscr{A}}{\partial z}\right) \\
\boldsymbol{\nabla}\times(\boldsymbol{v}\times\boldsymbol{B}) &= \hat{\boldsymbol{\varphi}}\left[\frac{\partial}{\partial z}\left(\Omega\frac{\partial\mathscr{A}}{\partial\varpi} - v_z B\right) - \frac{\partial}{\partial\varpi}\left(\Omega\frac{\partial\mathscr{A}}{\partial z} + v_\varpi B\right)\right] \\
&\quad + \frac{\hat{\boldsymbol{\varpi}}}{\varpi}\frac{\partial}{\partial z}\left(v_\varpi\frac{\partial\mathscr{A}}{\partial\varpi} + v_z\frac{\partial\mathscr{A}}{\partial z}\right) - \frac{\hat{\boldsymbol{z}}}{\varpi}\frac{\partial}{\partial\varpi}\left(v_\varpi\frac{\partial\mathscr{A}}{\partial\varpi} + v_z\frac{\partial\mathscr{A}}{\partial z}\right)\,. \qquad (2)
\end{aligned}
$$

To complete the equations we also need

$$
\begin{aligned}
\boldsymbol{\nabla}\times(A\boldsymbol{B}) &= \boldsymbol{\nabla}\times\left[\frac{\hat{\boldsymbol{\varphi}}(AB\varpi)}{\varpi} + A\boldsymbol{\nabla}\mathscr{A}\times\frac{\hat{\boldsymbol{\varphi}}}{\varpi}\right] \\
&= \boldsymbol{\nabla}(AB\varpi)\times\frac{\hat{\boldsymbol{\varphi}}}{\varpi} + \frac{\hat{\boldsymbol{\varphi}}\cdot\boldsymbol{\nabla}(A\boldsymbol{\nabla}\mathscr{A})}{\varpi} - \frac{\hat{\boldsymbol{\varphi}}\boldsymbol{\nabla}\cdot(A\boldsymbol{\nabla}\mathscr{A})}{\varpi} - A\boldsymbol{\nabla}\mathscr{A}\cdot\boldsymbol{\nabla}\left(\frac{\hat{\boldsymbol{\varphi}}}{\varpi}\right) \\
&= \boldsymbol{\nabla}(AB\varpi)\times\frac{\hat{\boldsymbol{\varphi}}}{\varpi} + \frac{2\hat{\boldsymbol{\varphi}}A}{\varpi^2}\frac{\partial\mathscr{A}}{\partial\varpi} - \frac{\hat{\boldsymbol{\varphi}}\boldsymbol{\nabla}\cdot(A\boldsymbol{\nabla}\mathscr{A})}{\varpi} \\
\boldsymbol{\nabla}\times(\eta\boldsymbol{\nabla}\times\boldsymbol{B}) &= \boldsymbol{\nabla}\eta\times\boldsymbol{\nabla}\times\boldsymbol{B} + \eta\boldsymbol{\nabla}\times(\boldsymbol{\nabla}\times\boldsymbol{B}) \\
\boldsymbol{\nabla}\times(\boldsymbol{\nabla}\times\boldsymbol{B}) &= -\boldsymbol{\nabla}\left[\varpi\frac{\partial}{\partial\varpi}\left(\frac{1}{\varpi}\frac{\partial\mathscr{A}}{\partial\varpi}\right) + \frac{\partial^2\mathscr{A}}{\partial z^2}\right]\times\frac{\hat{\boldsymbol{\varphi}}}{\varpi} \\
&\quad + \hat{\boldsymbol{\varphi}}\left[-\frac{\partial^2 B}{\partial z^2} - \frac{\partial}{\partial\varpi}\left(\frac{1}{\varpi}\frac{\partial(B\varpi)}{\partial\varpi}\right)\right]\,. \qquad (3)
\end{aligned}
$$

Dyda, Lovelace, Ustyugova, Koldoba, Wasserman 2015

Simulations of Disc Dynamo

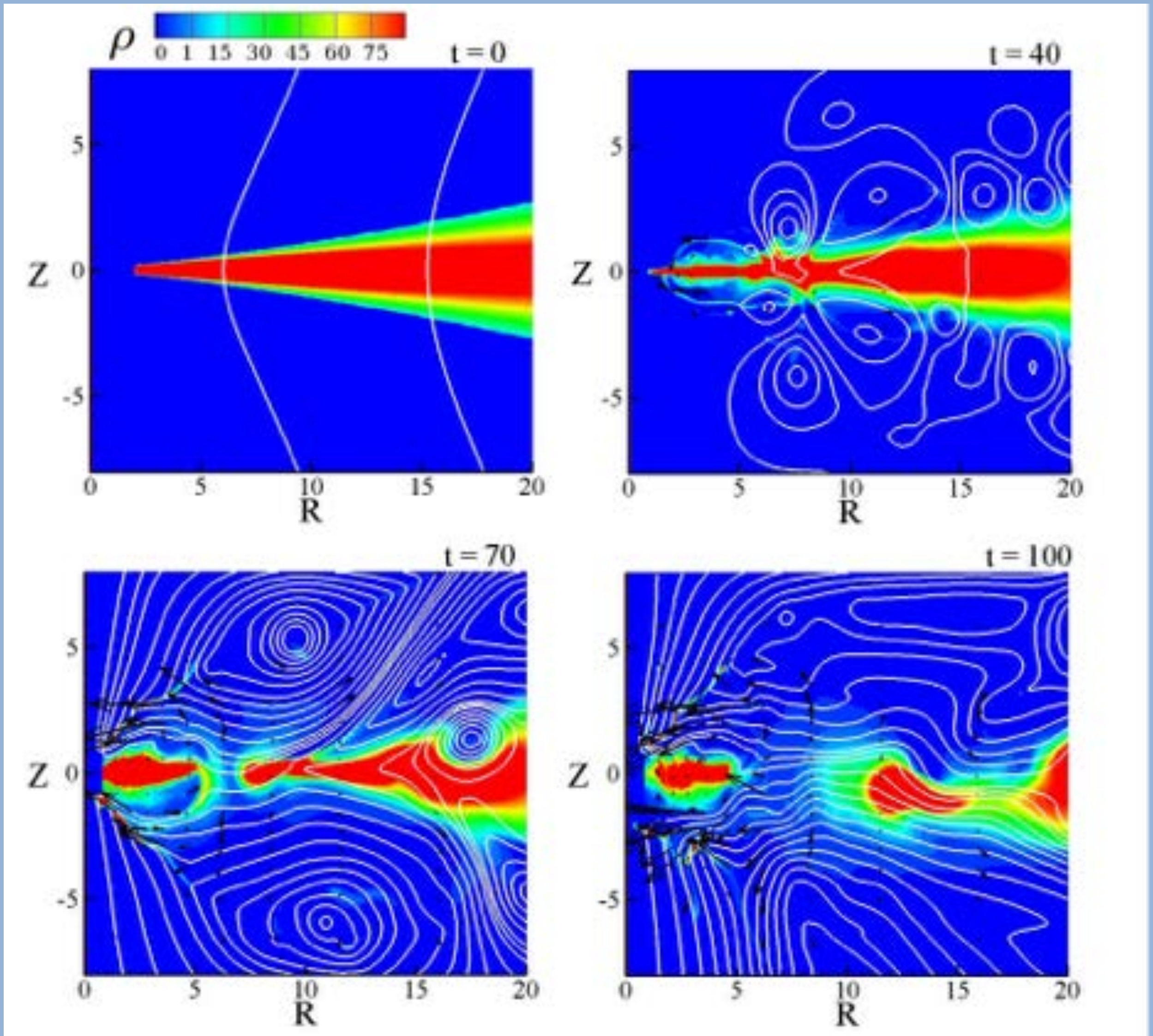

Dyda, Lovelace, Ustyugova, Koldoba, Wasserman 2015

Magneto-Rotational Instability (MRI)

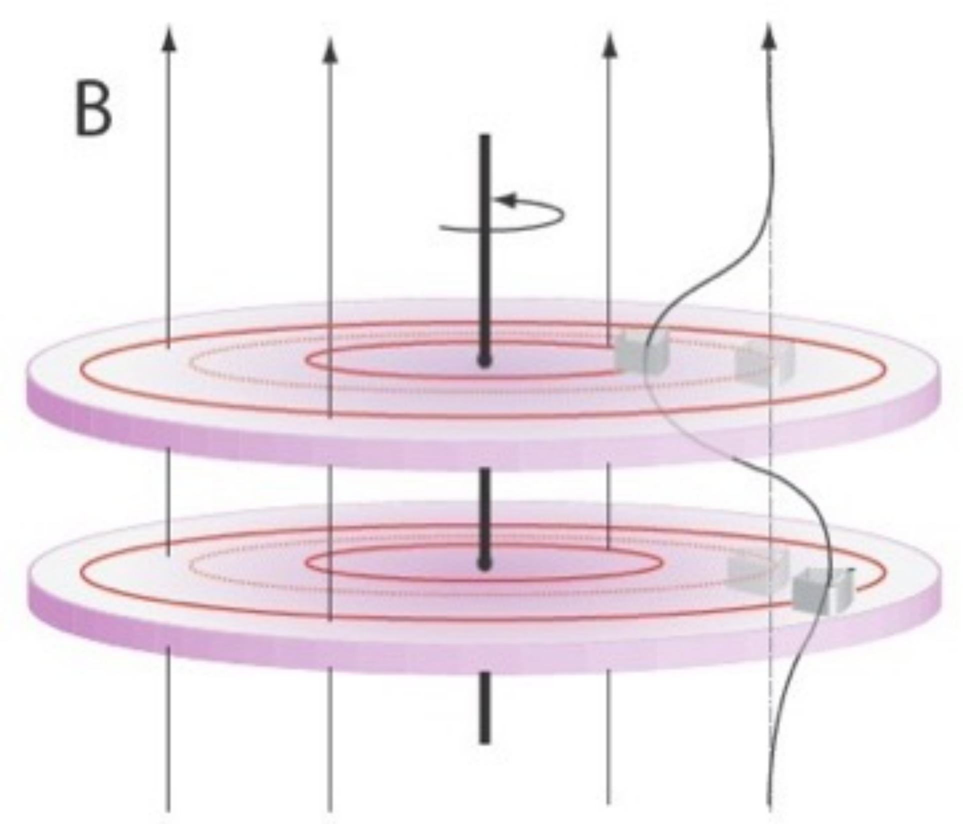

Velikhov 1959, Chandrasekhar 1961, Balbus & Hawley 1991

- Magnetic field lines are stretched by the differential rotation
- The toroidal field increases
- Reconnection, turbulence

3D Simulations of MRI-driven Accretion onto Magnetized Stars

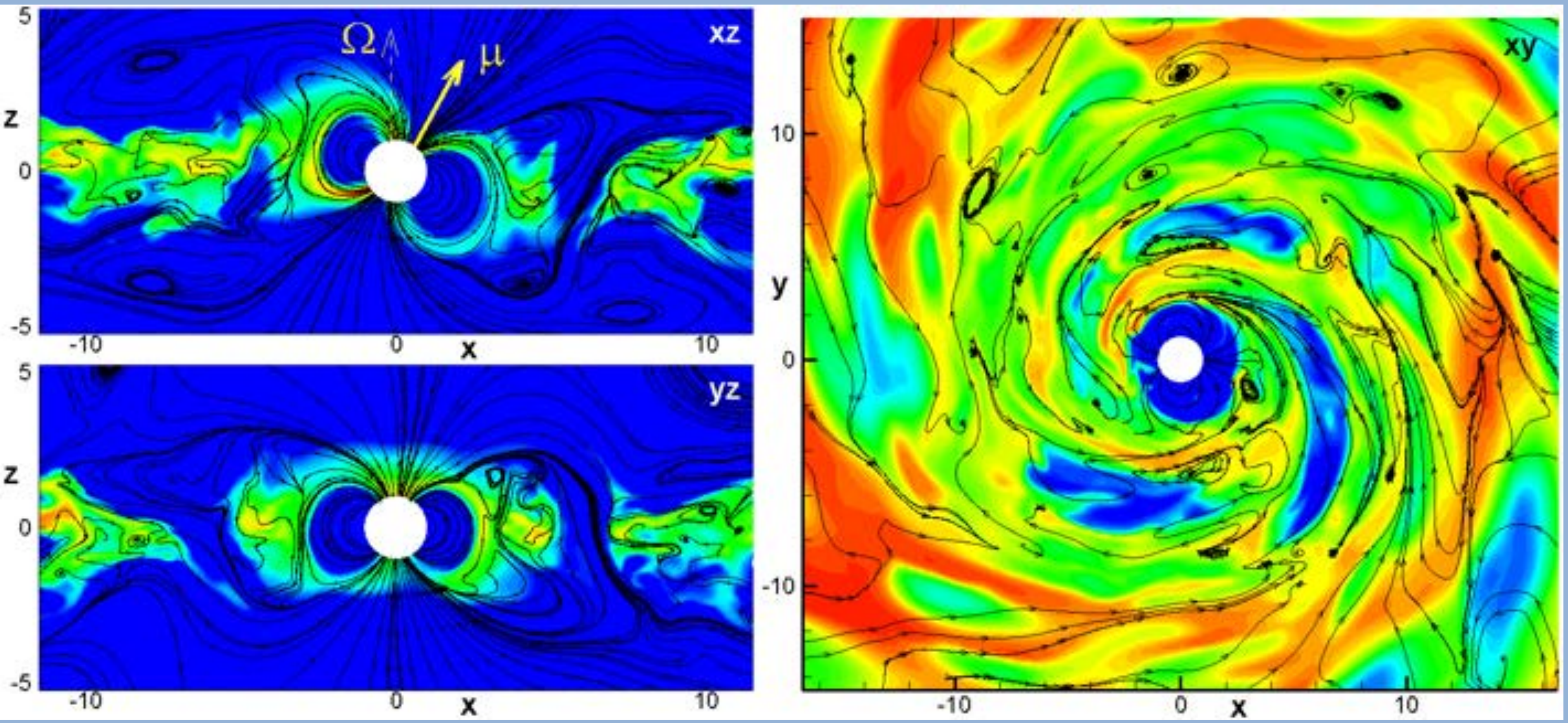

- Matter accretes in funnel streams
- Matter in the disk forms elongated turbulent cells

2.5D Simulations of MRI-driven Accretion

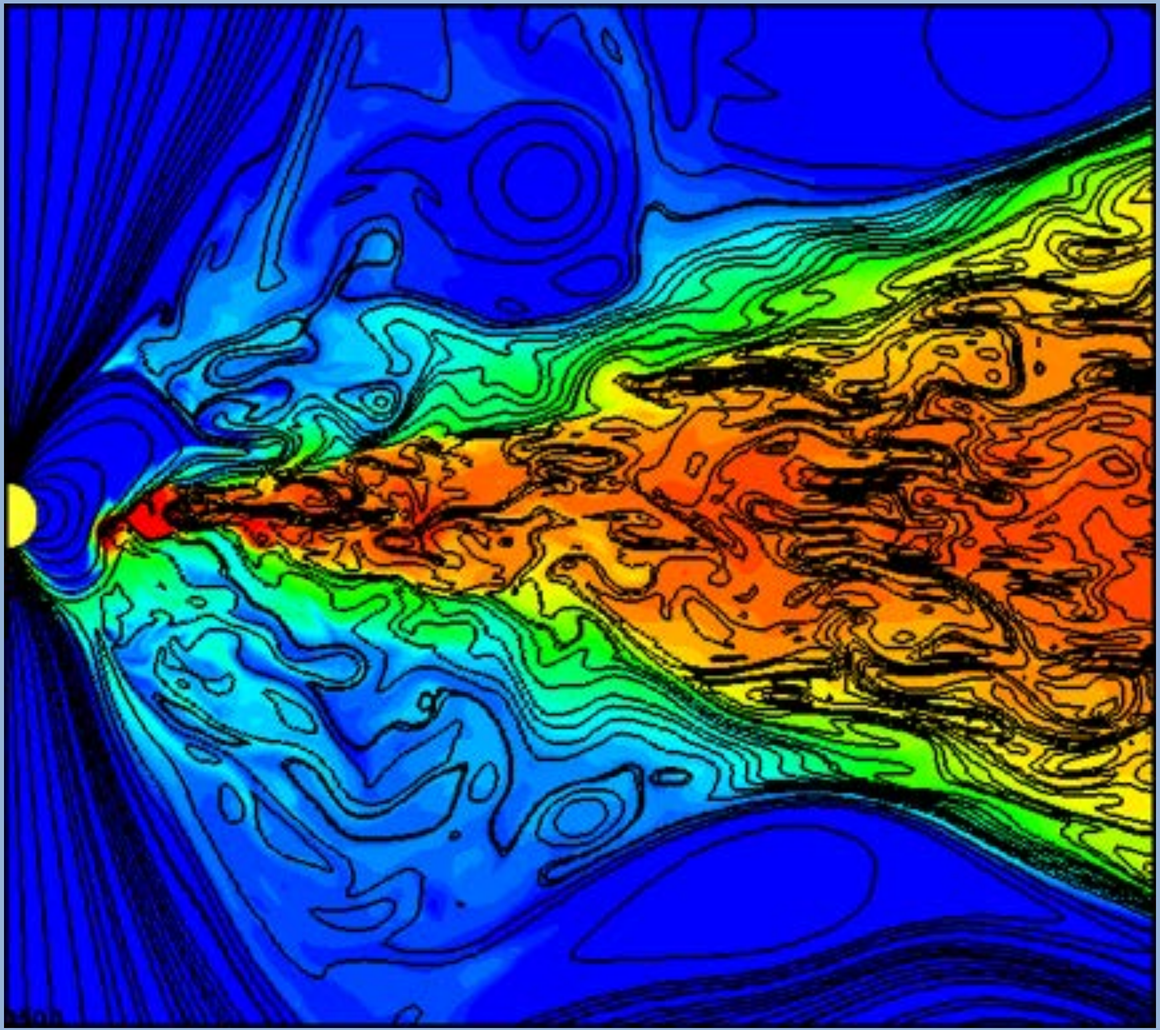

- Matter in the disk forms elongated turbulent cells
- There are current sheets between turbulent cells

2.5D Simulations of MRI-driven Accretion

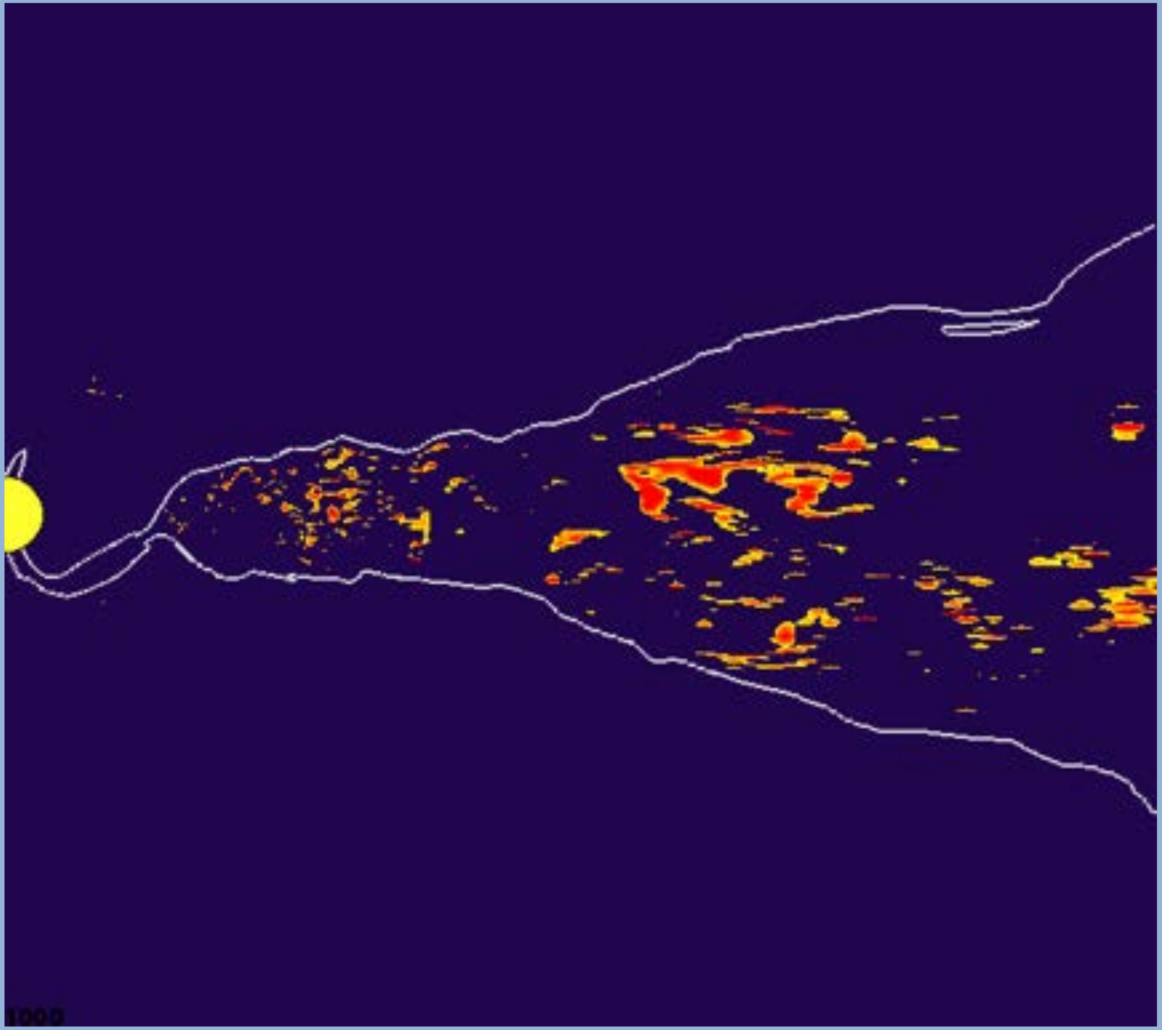

- The color background shows currents
- Reconnection, flares are expected

II. 3D Simulations of Accretion onto Magnetized Stars

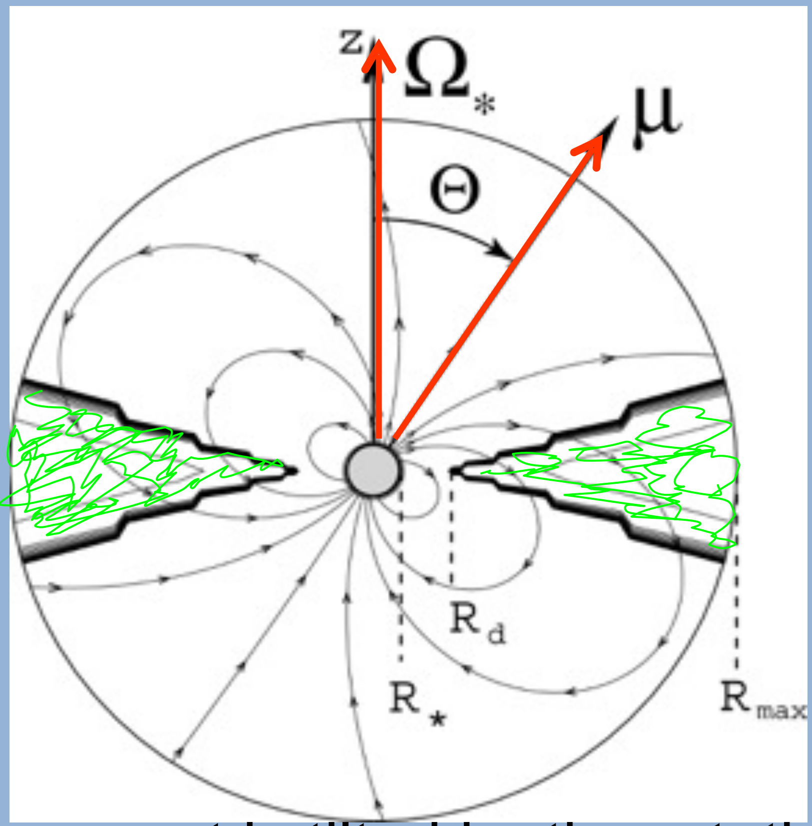

- The dipole moment is tilted by the rotational axis at an Θ
- Disk is dense and cold
- Corona is low-density and hot

Romanova, Ustyugova, Koldoba, Lovelace 2003, 2004

"Cubed sphere" grid

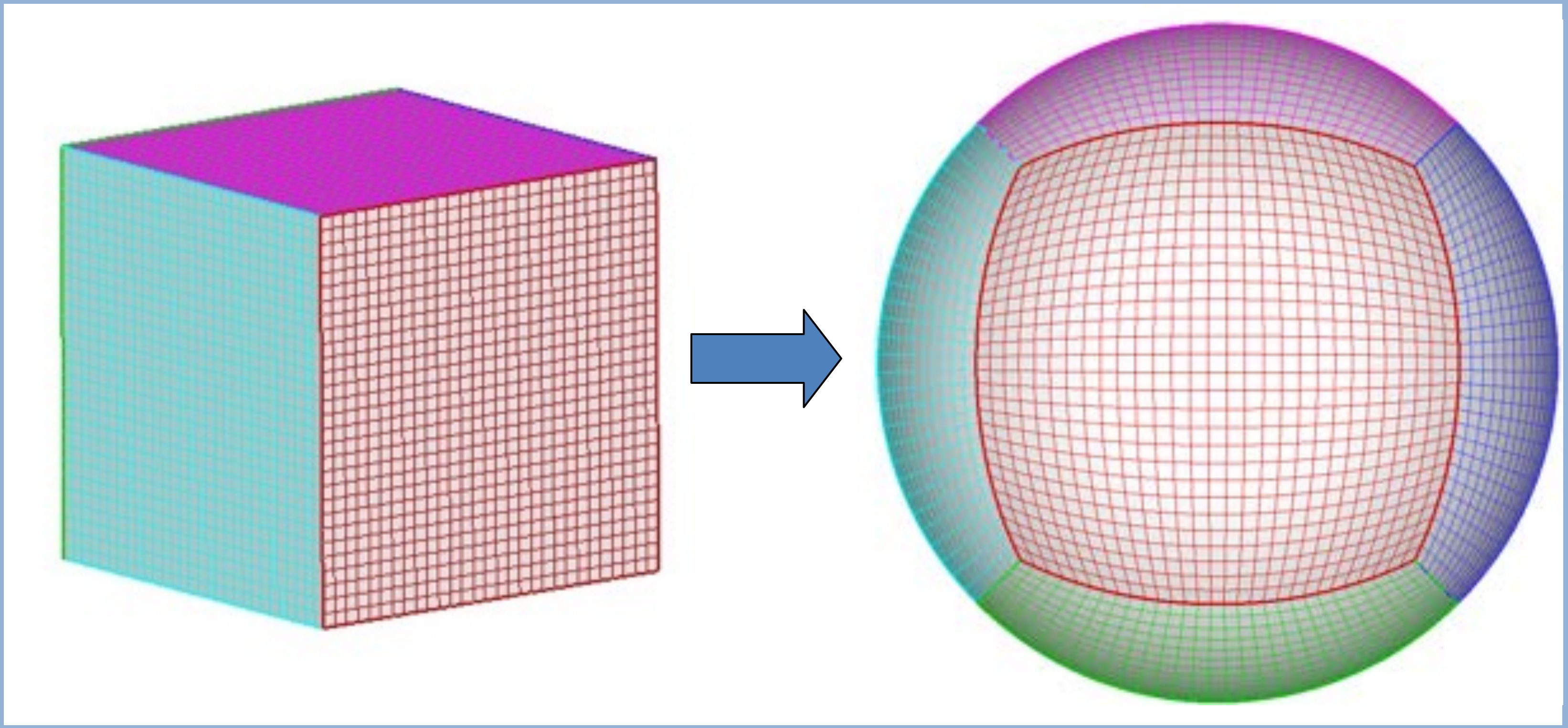

- Each sphere is an inflated cube
- Set of cubed spheres

1 block: 80x31x31 – spherical: 80x62x124
1 block: 120x51x51 – spherical: 120x102x204

- Has advantages over Cartesian and spherical grids
- High resolution in the center, where star is located

Koldoba, Romanova, Ustyugova, Lovelace 2002,2015

MHD Equations:

- Written in the coordinate system rotating with the star
- Splitting of the field: B = $B_0 + B_1$ (*Tanaka 1994*)

$$\frac{\partial \rho}{\partial t} + \nabla \cdot (\rho \boldsymbol{v}) = 0 \quad (1)$$

$$\frac{\partial \rho \boldsymbol{v}}{\partial t} = -\nabla \mathcal{T} + \rho\, \boldsymbol{g} + \underline{2\rho \boldsymbol{v} \times \boldsymbol{\Omega} - \rho \boldsymbol{\Omega} \times (\boldsymbol{\Omega} \times \boldsymbol{R})} \quad (2)$$

$$\frac{\partial (\rho S)}{\partial t} + \nabla \cdot (\rho \boldsymbol{v} S) = Q \quad (3)$$

$$\frac{\partial \boldsymbol{B}}{\partial t} + \nabla \times (\boldsymbol{B} \times \boldsymbol{v}) = \eta \nabla^2 \boldsymbol{B} \quad (4)$$

$$\nabla \cdot \boldsymbol{B} = 0$$

Corotating frame

Heat equation

Diffusivity (2D)

Stress tensor, viscosity

Disk-Magnetosphere Interaction

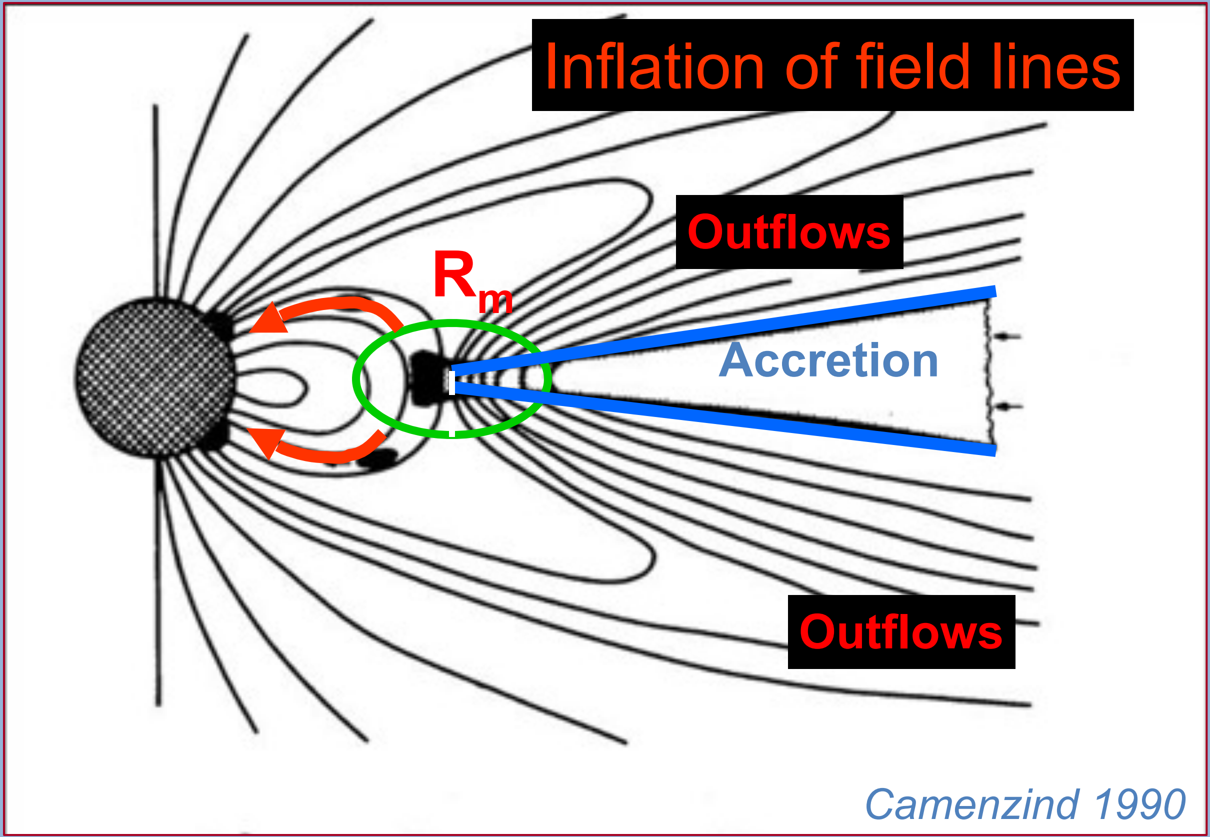

Magnetospheric accretion: Pringle & Rees 1972; Gosh & Lamb 1978, 1979; Uchida & Shibata 1985; Konigl 1990; Cameron & Campbell 1993; Romanova et al. 2002-2004; Long et al. 2005; Bessolaz et al. 2007; Kluzniak & Rappaport 2007

Inflation and Outflows: Lovelace et al. 1995; Miller & Stone 1997; Goodson et al. 1997,1999; Elsner & Fendt 1999; Agapitou & Papaloizou 2000

Instabilities: Arons & Lea 1976; Kaisig, Tajima & Lovelace 1992; Spruit et al. 1993, 1995; Li & Narayan 2004; Romanova, Kulkarni & Lovelace 2008; Kulkarni & Romanova 2008, 2009

First 3D simulations (inner 1/5 region)

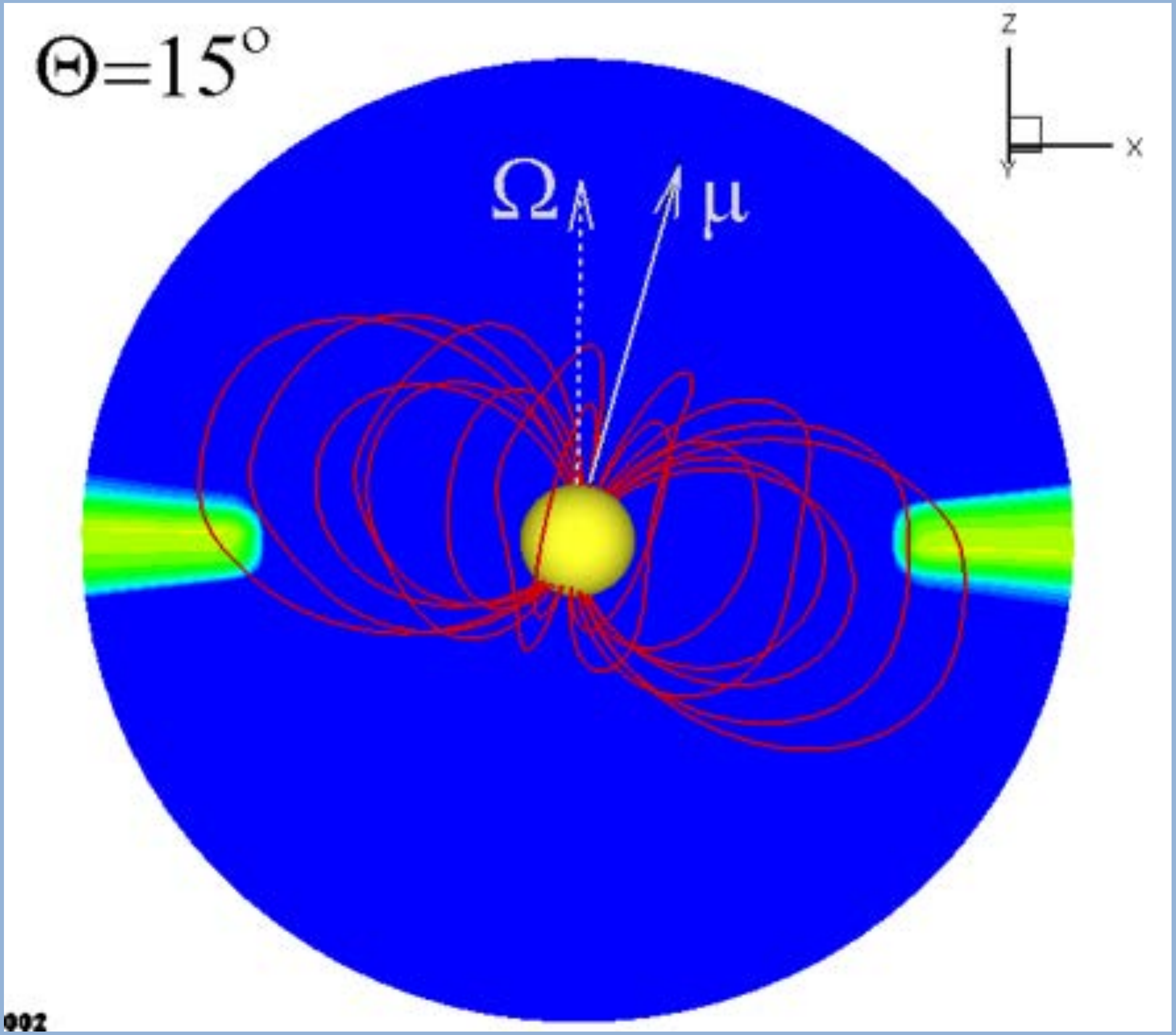

XZ-slice and 3D field lines

Matter is stopped by magnetosphere and accretes in funnel streams

Romanova, Ustyugova, Koldoba, Lovelace 2003, 2004

Different features in the disk and magnetosphere

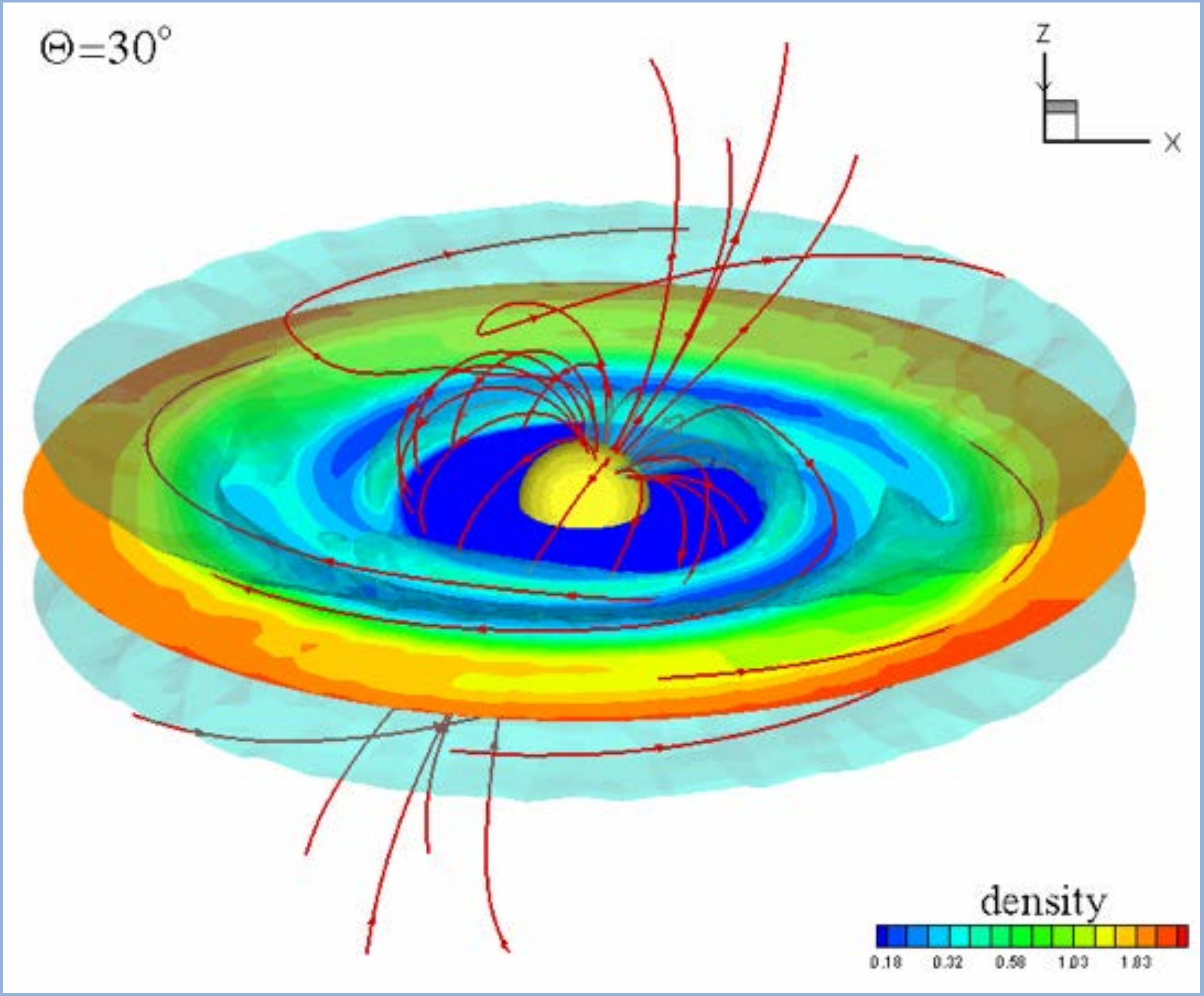

Funnel Streams, Hot Spots

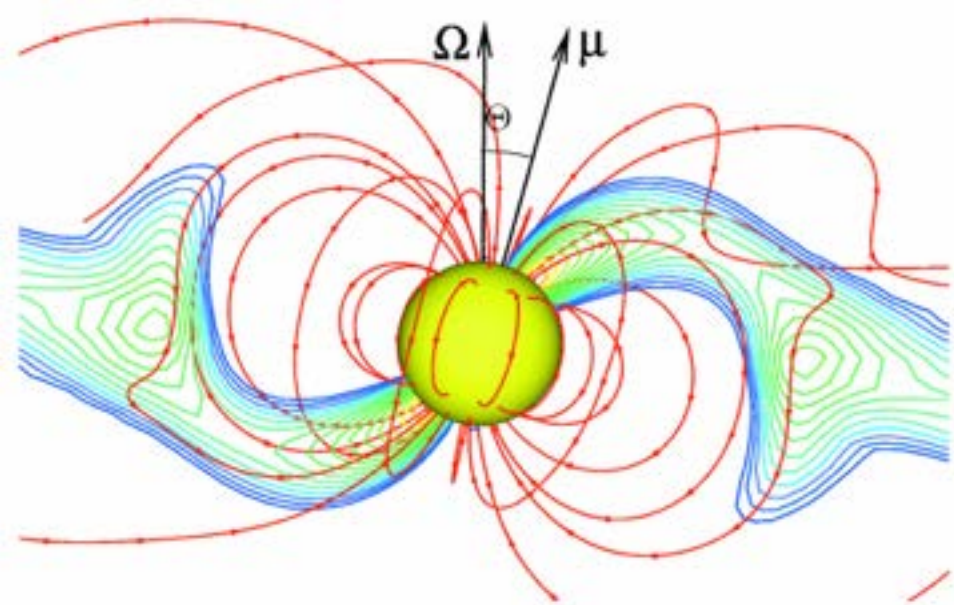

Hot Spot

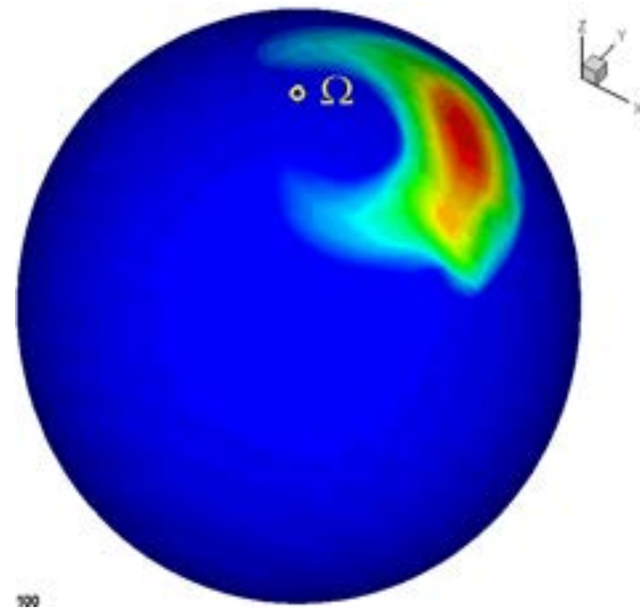

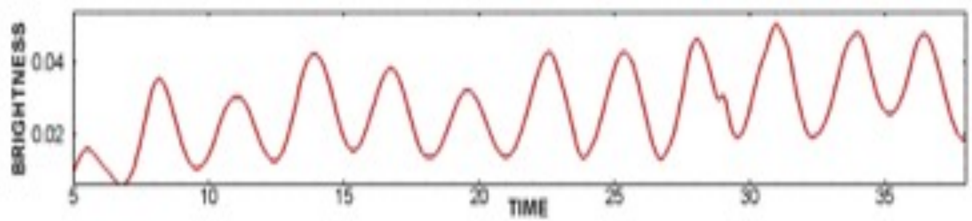

Light Curve

Romanova, Ustyugova, Koldoba, Lovelace 2004

Numerical Discovery: Two Regimes of Accretion

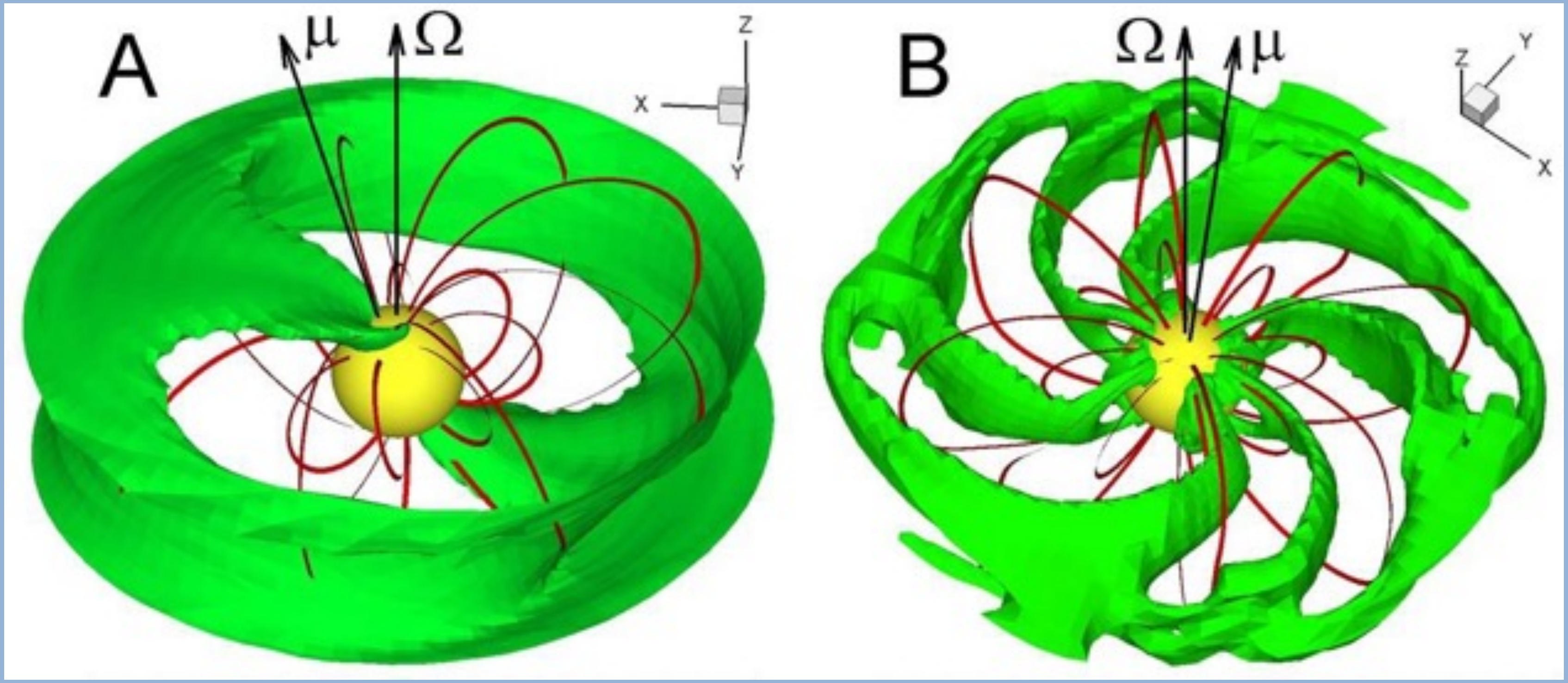

Stable regime of accretion

Unstable regime of accretion

Kulkarni & Romanova 2008, 2009; Romanova, Kulkarni & Lovelace 2008

Magnetic Interchange Instability

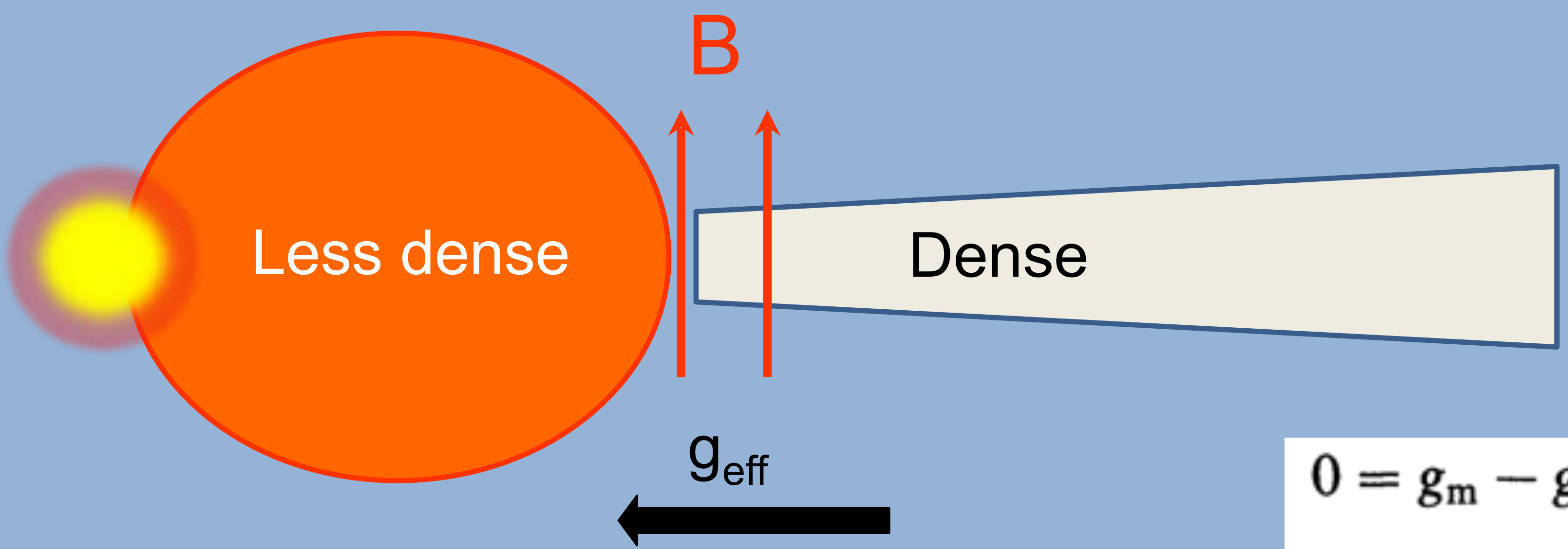

$$0 = g_m - g + \Omega^2 r,$$

where

$$g_m = \frac{B_r^+ B_z}{2\pi\Sigma}$$

$$\boxed{\gamma_{B\Sigma}^2 \equiv g_{eff} \left| \frac{d}{dr} \ln \frac{\Sigma}{B_z} \right| > 2 \left(r \frac{d\Omega}{dr} \right)^2 \equiv \gamma_\Omega^2}$$

$g_{eff} = g - \Omega^2 r$

$r \frac{d\Omega}{dr}$ Shear in the disk acts to suppress the instability

Kaisig, Tajima, Lovelace 1992, Spruit et al. 1995

First Application to Accretion Disks

THE ASTROPHYSICAL JOURNAL, 386:83–89, 1992 February 10

MAGNETIC INTERCHANGE INSTABILITY OF ACCRETION DISKS

M. KAISIG,[1] T. TAJIMA,[1] AND R. V. E. LOVELACE[1,2]

Received 1991 March 18; accepted 1991 August 7

ABSTRACT

A study is made of the nonlinear evolution of the magnetic interchange or buoyancy instability of a differentially rotating disk threaded by an ordered vertical magnetic field. As a model for the disk we consider a two-dimensional ideal fluid in the equatorial plane of a central mass in the corotating frame of reference. We use a local approximation of a shearing sheet and study the evolution numerically by solving the equations of ideal magnetohydrodynamics.

If the rotation rate of the disk is Keplerian, the disk is found to be stable. If the vertical magnetic field is sufficiently strong, and the field strength decreases with distance from the central object, and thus the rotation of the disk deviates from Keplerian, we find that an instability develops. The magnetic flux and disk matter expand outward in certain ranges of azimuth, while disk matter with less magnetic flux moves inward over the remaining range of azimuth, showing a characteristic development of an interchange instability. Saturation and eventually decay occur when the field enters the outer Keplerian part of the disk. The growth rate ω_i in the initial, linear regime depends on the azimuthal wavenumber k of the initial perturbation as $\omega_i \sim k^{1/2}$. The growth rate decreases as $\beta = 4\pi p/B^2$ increases and vanishes for $\beta > 5$.

When a slow but steady supply of vertical magnetic field is present in the accretion flow, the magnetic perturbation persists and gives rise to a steady state disk configuration in which there is an outward angular momentum transport which corresponds to a dimensionless viscosity (Shakura-Sunyaev) parameter of $\alpha \sim 0.1$.

Subject headings: accretion, accretion disks — instabilities — MHD

Ordered vertical magnetic field threads the disk

Magnetic Interchange Instability

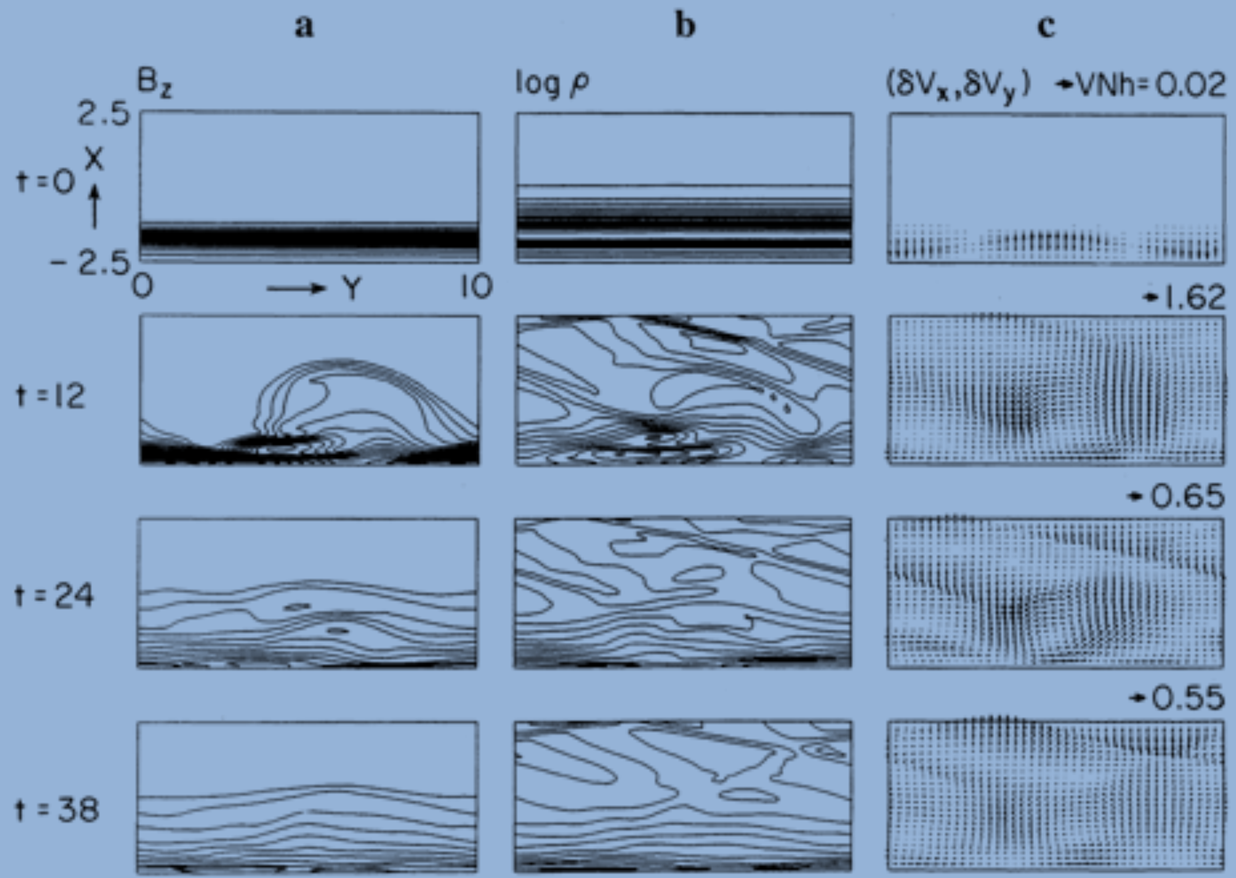

FIG. 1.—Numerical results for four different time steps: (*a*) the contour lines of B_z, (*b*) the density contours (log ρ), and (*c*) the velocity perturbation (δV_x, δV_y). Total illustrated area is (5 × 10) in units of h_0. The contour level step width is 0.9 for (*a*) in units of linear scale and 0.2 for (*b*) in units of logarithmic scale. The scale *VNh* of the velocity vector is shown at the top of the figure in (*c*) in units of the isothermal speed of sound. Numbers in the left-hand-side of each frame in (*a*) represent the time in units of the Keplerian period.

An example of numerical simulations of interchange instability

From: Kaisig, Tajima & Lovelace 1992

Matter “sneaks” between the field lines

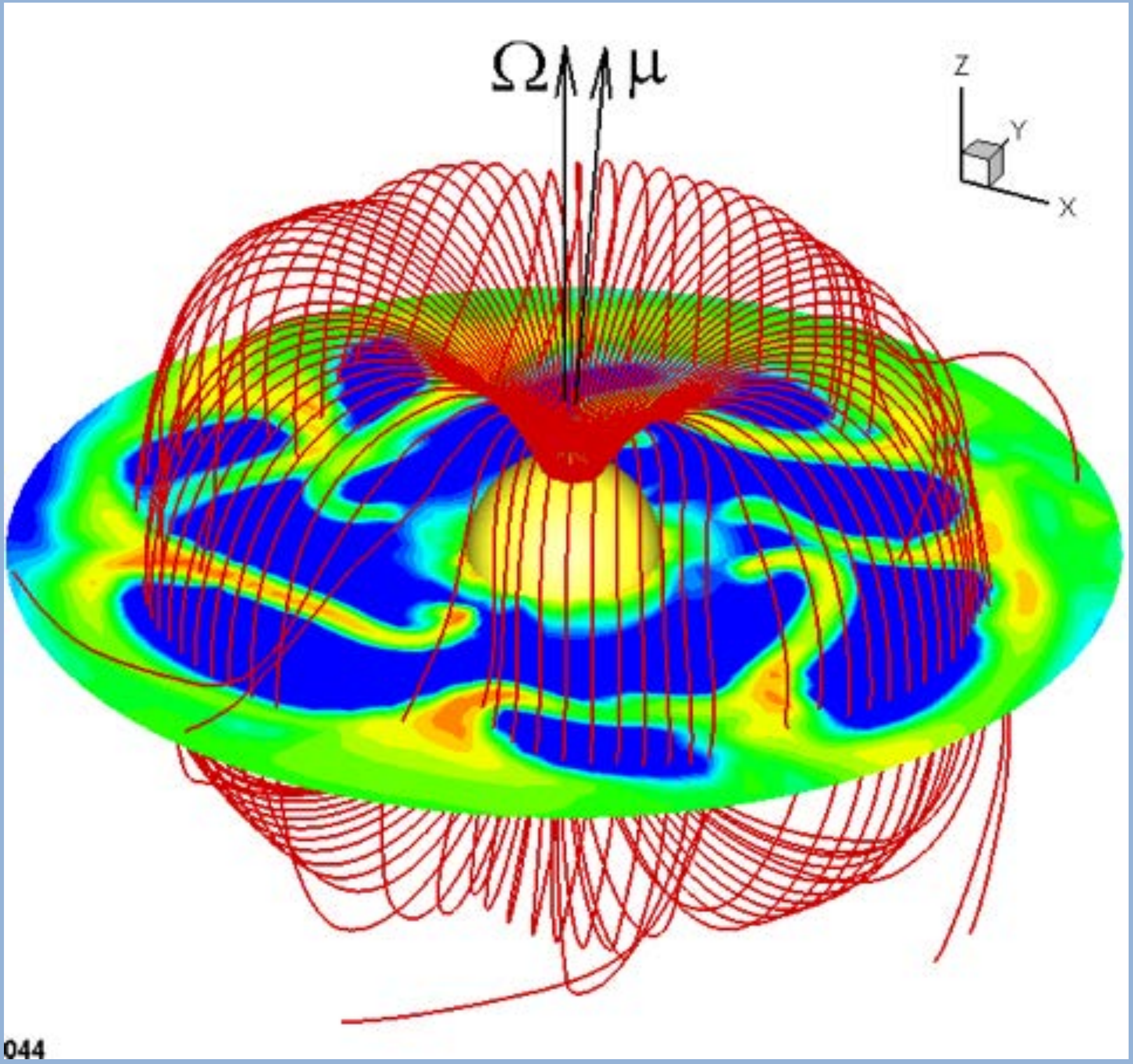

Stereo Animations

RED -- left
BLUE -- right

IF YOU WEAR GLASSES then PUT THE STEREOSCOPIC GLASSES ON TOP OF THEM

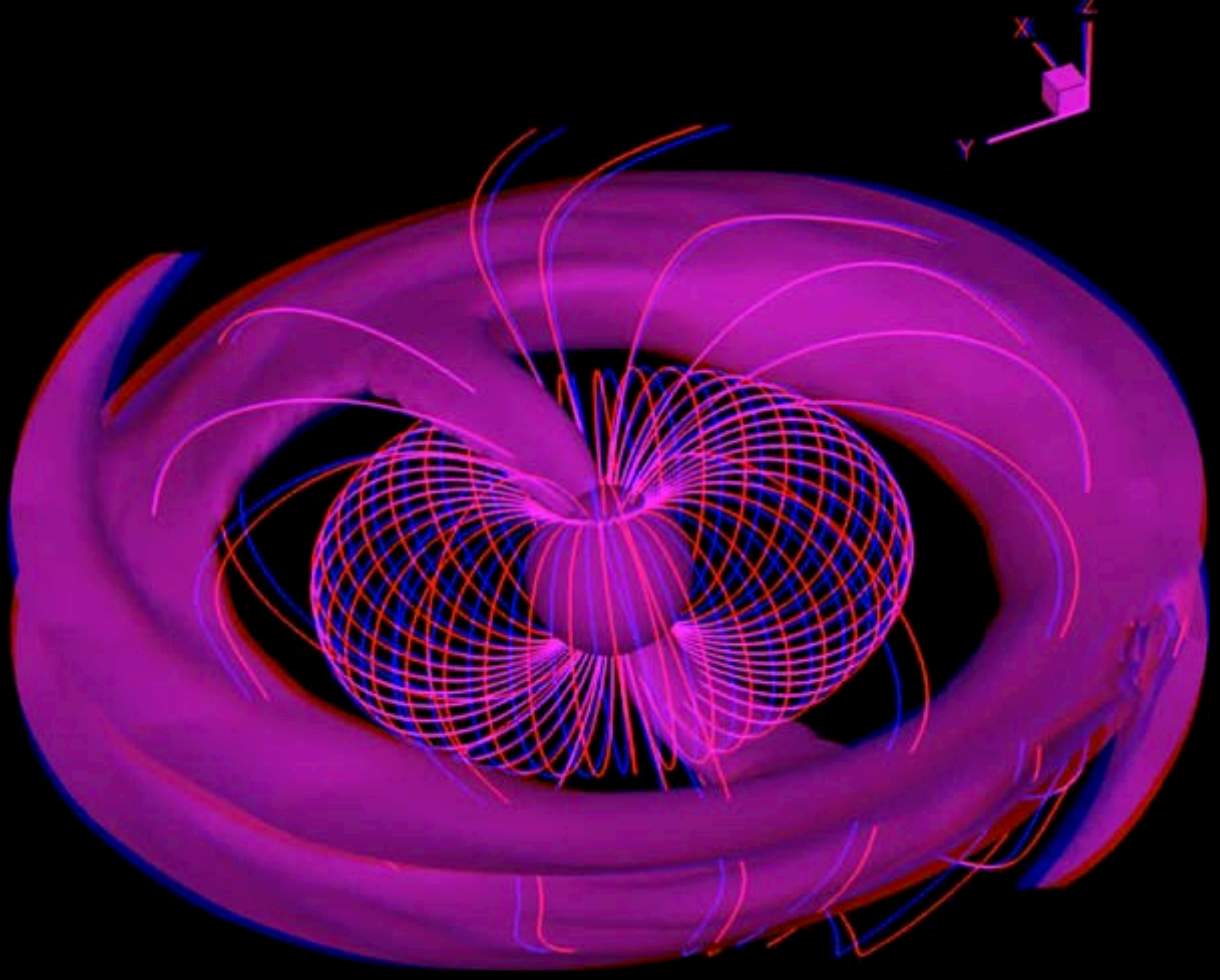
X
Y
Z

Z
Y
Ω

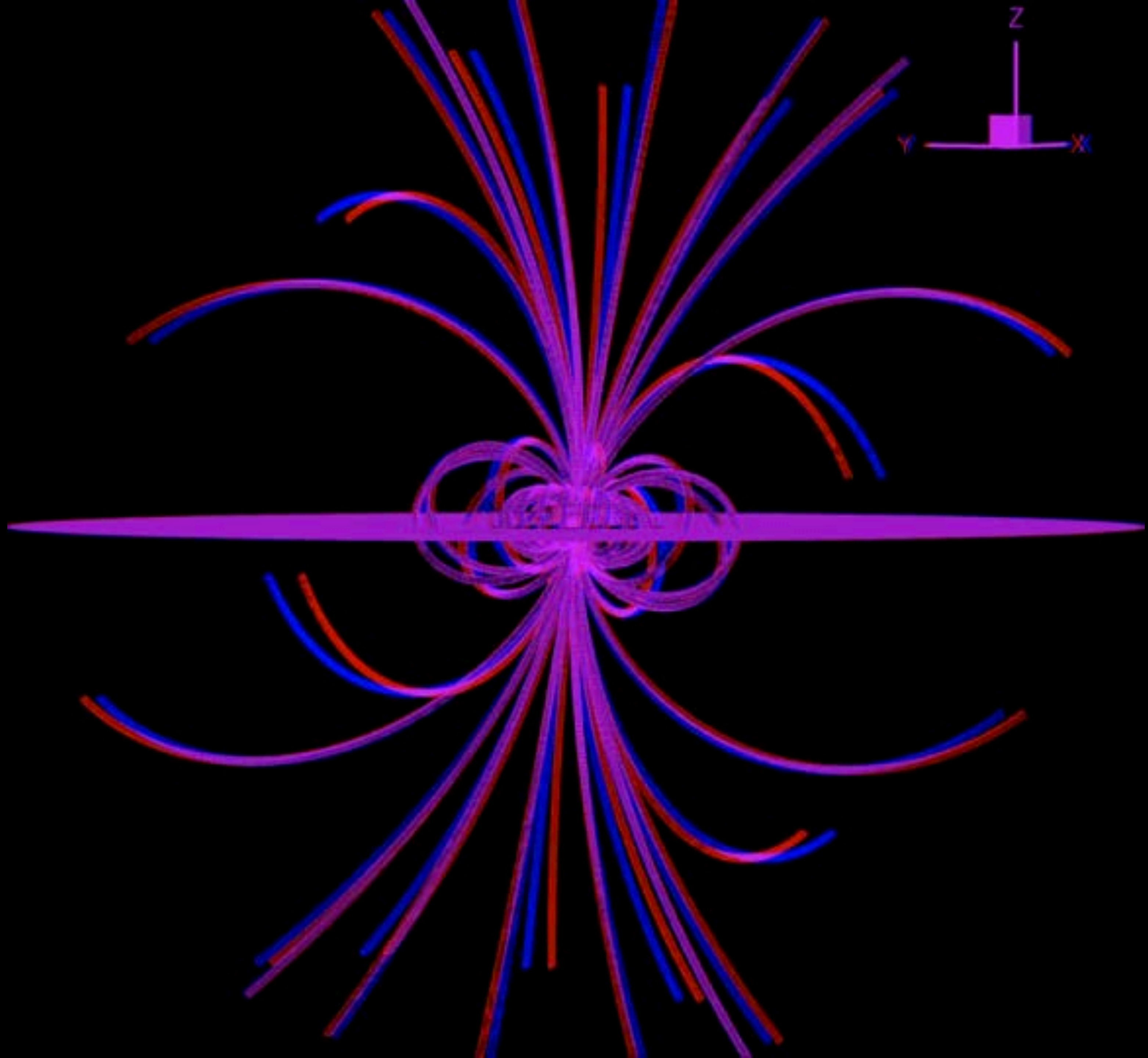
Z
Y
X

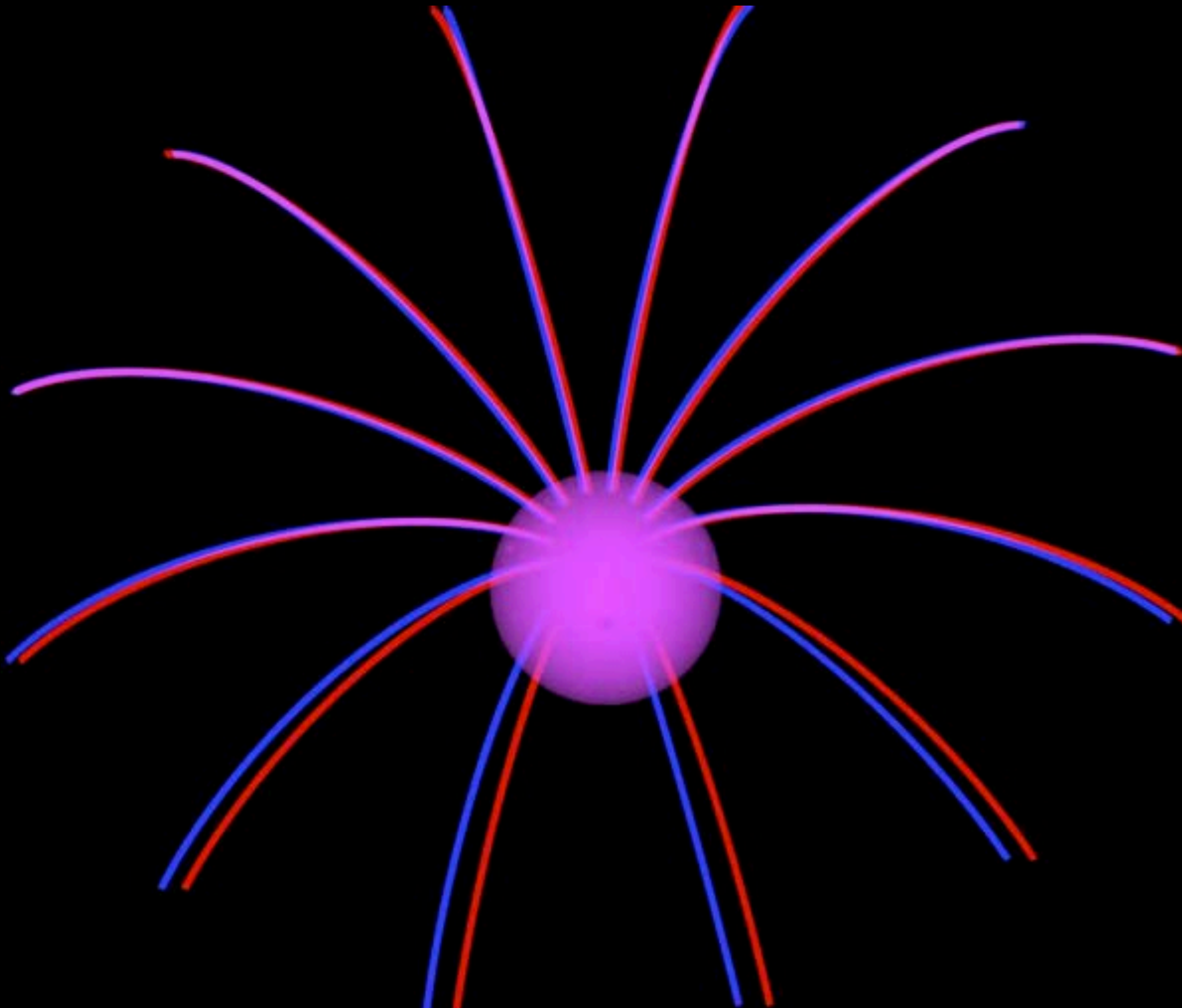

III. Outflows: Problem of Launching

Gravity attracts. How to launch jets ?

Magnetic Force Drives Outflows

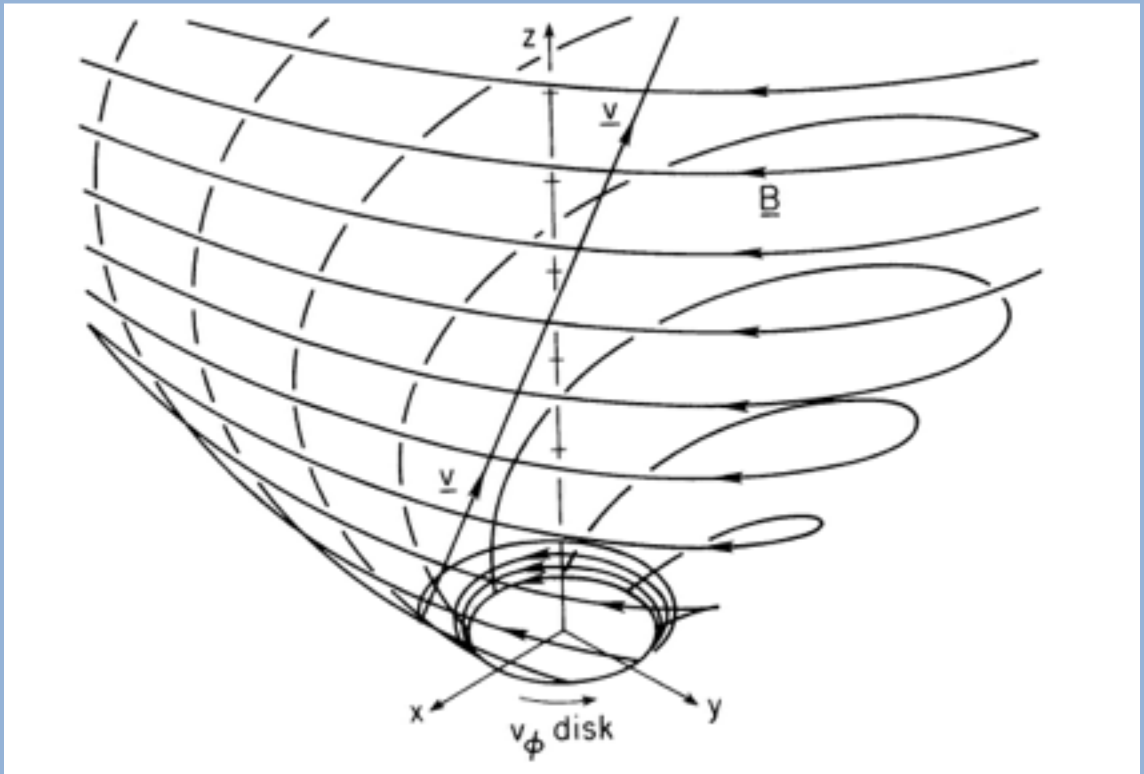

Lovelace, Berk, Contopoulos 1991

- Azimuthal magnetic field is generated by rotating disk
- Magnetic pressure gradient drives the outflows
- Magnetic force also collimated the jet

Simulations of Magnetically-driven Winds

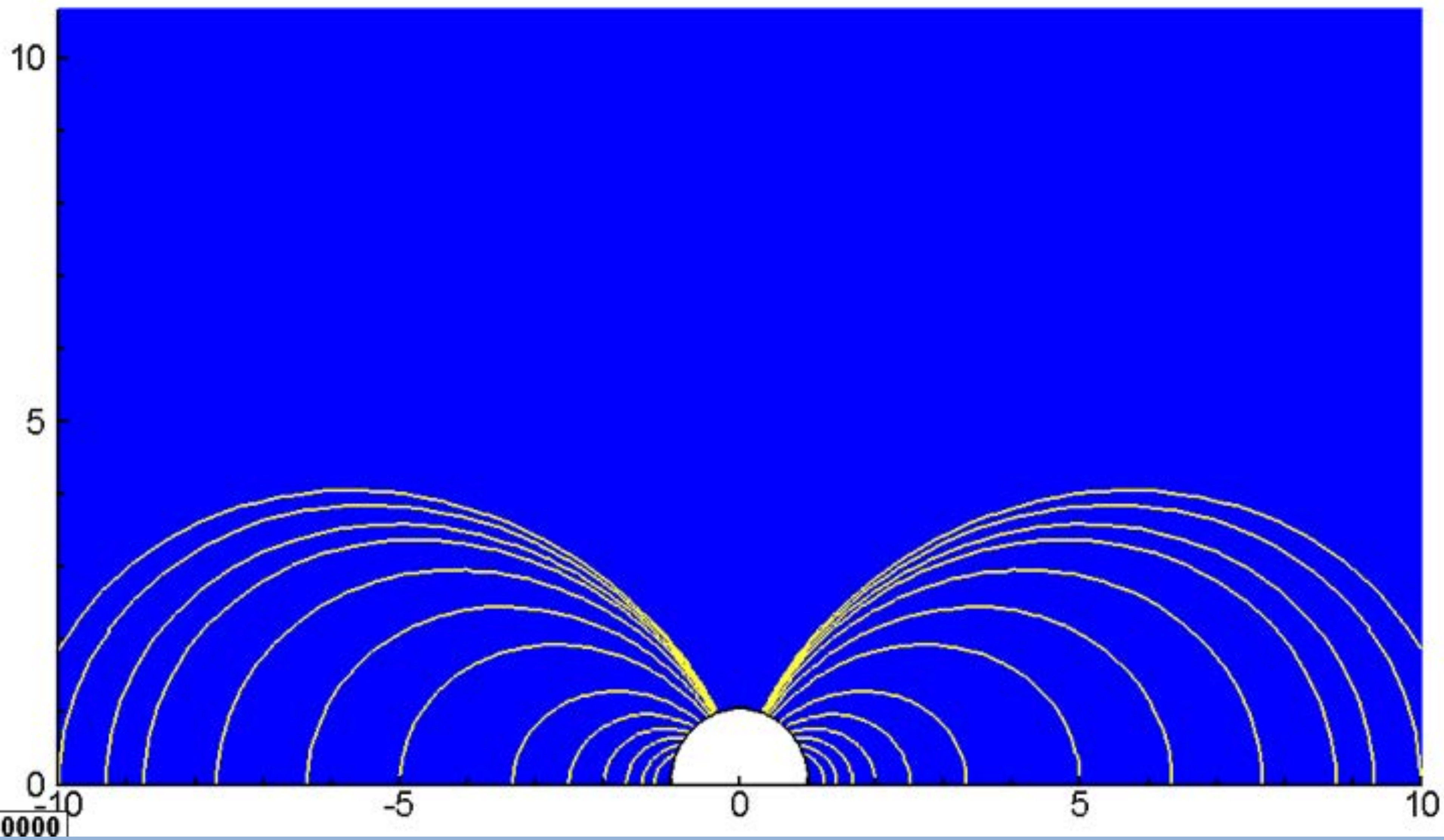

$\dot{M}_{wind} = 0.2 – 0.3\ \dot{M}_{star}$

Romanova et al. 2009

Poloidal current: $I_p = rB_\phi$

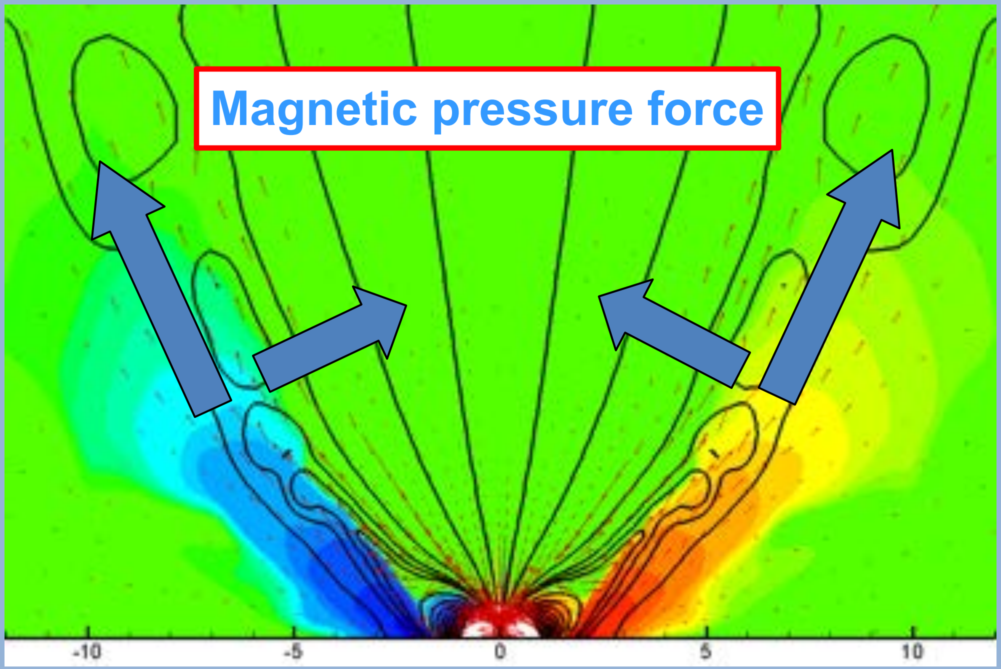

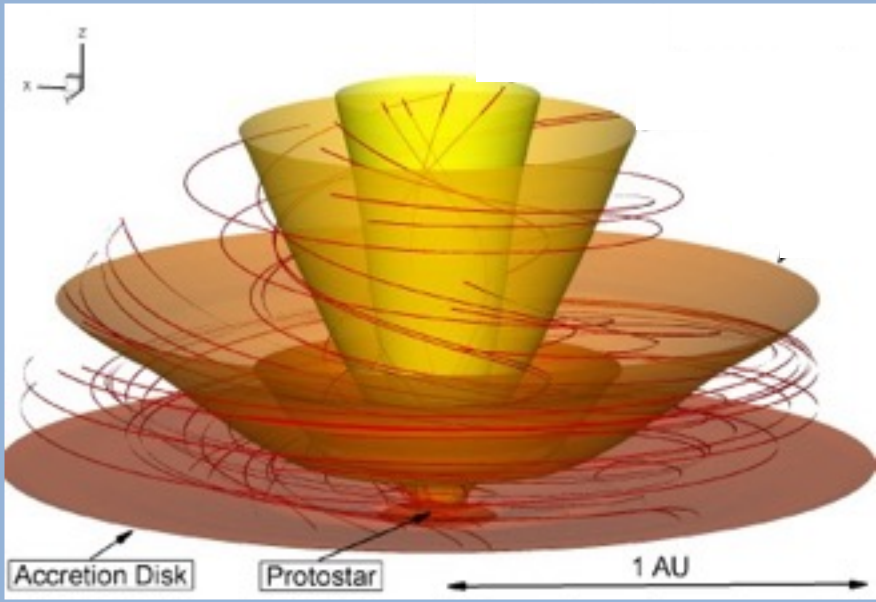

Magnetic force: *Lovelace et al. 1991*

3D rendering: azimuthal component

Driving force is the magnetic force:

$$F_m = -k \nabla (rB_\phi)^2$$

Magnetic force determines both: acceleration and collimation

Propeller Regime: Centrifugal Force

$$\boxed{r_m > r_{cor}}$$

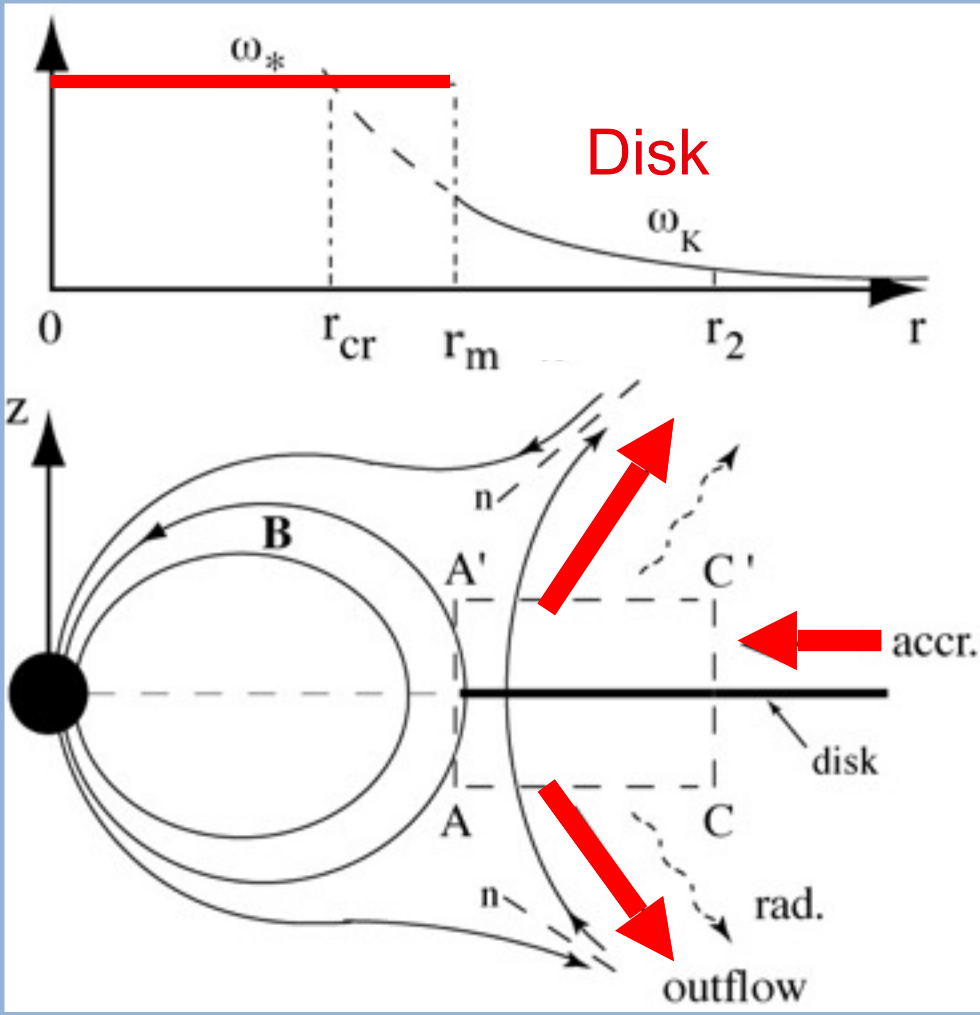

Lovelace, Romanova and Bisnovatyi-Kogan 1999
Illarionov & Sunyaev 1975;

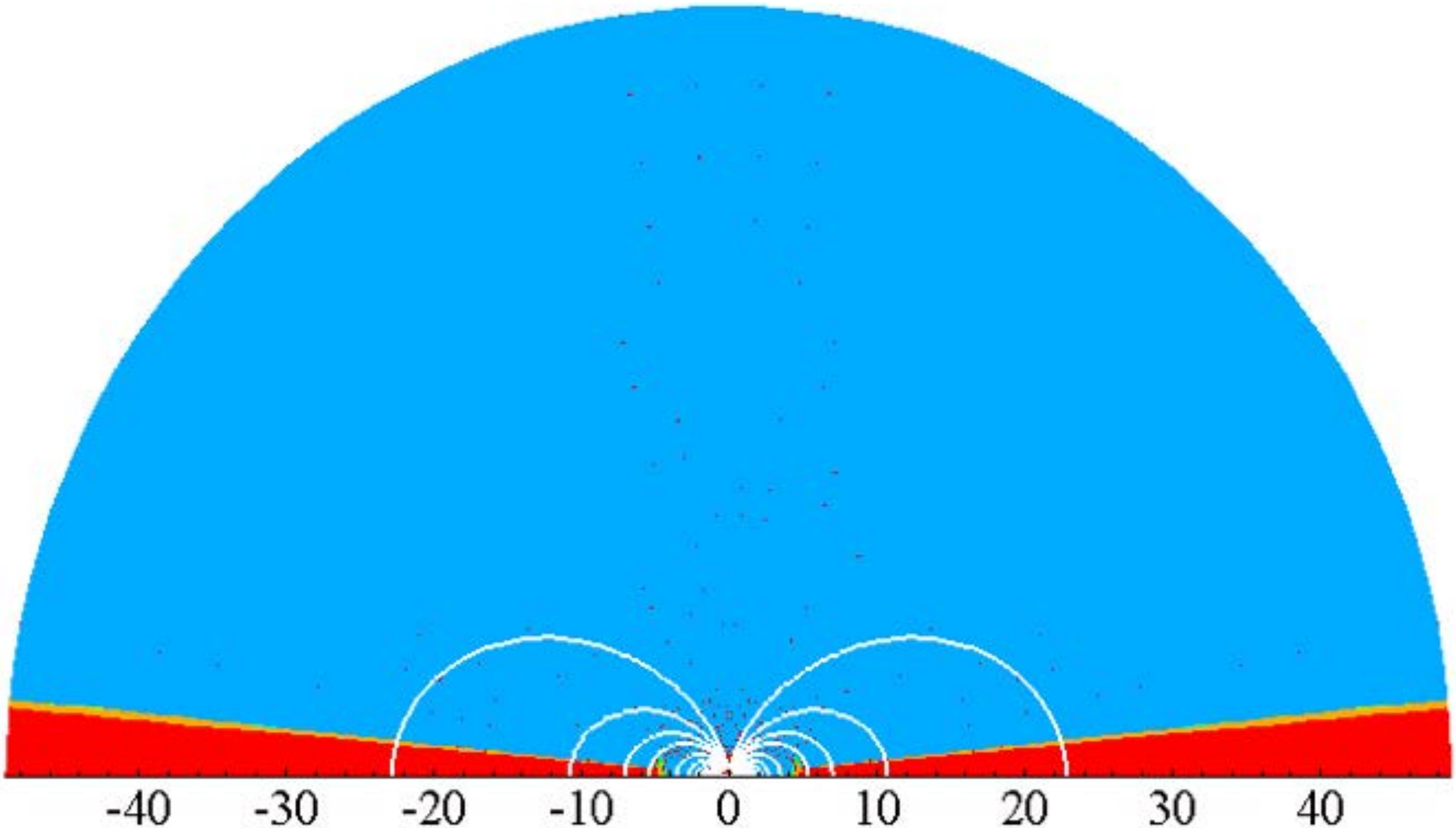

-40
-30
-20
-10
0
10
20
30
40

Two-component Outflows

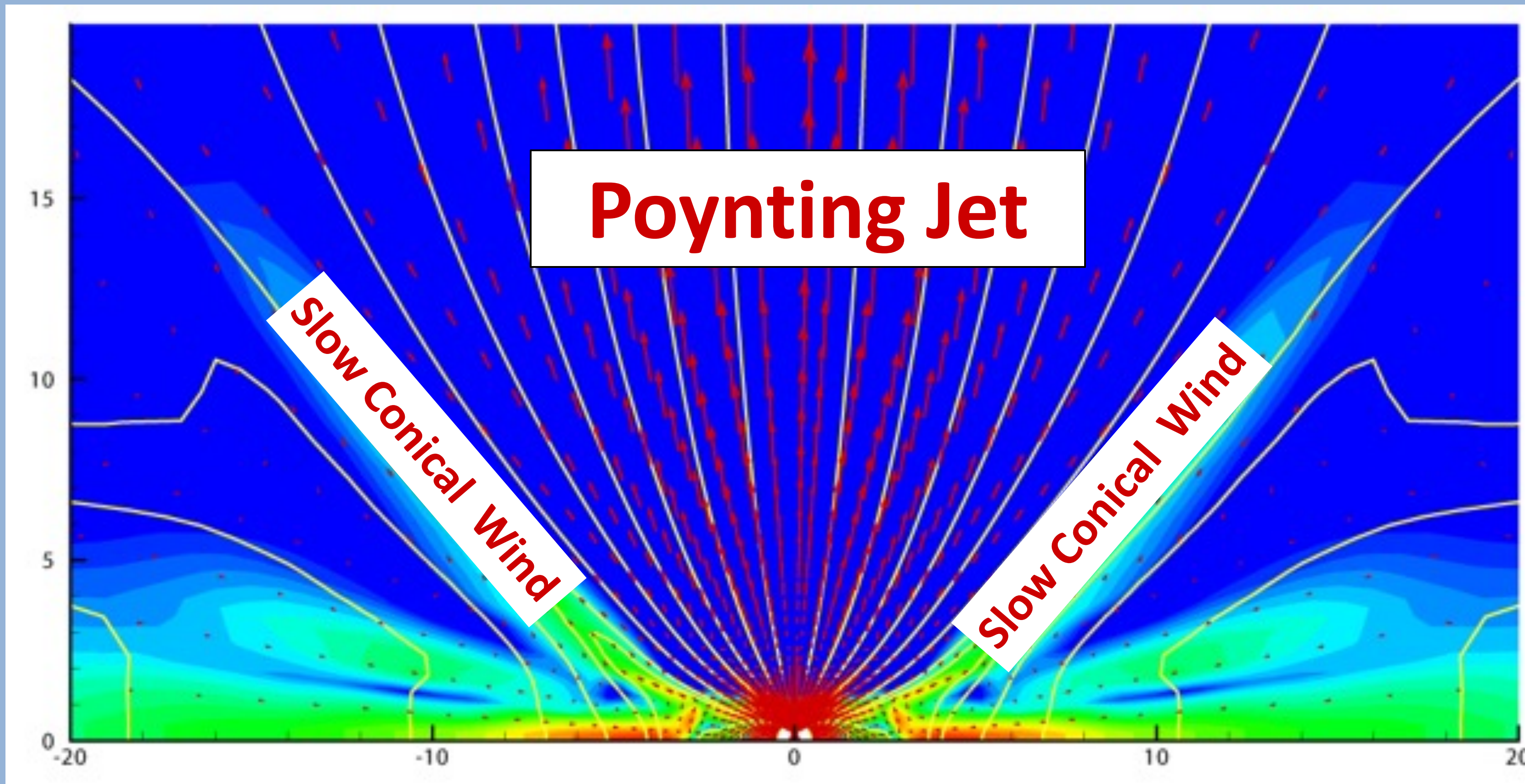

- Conical winds carry most of matter outwards
- Poynting jet carries energy and angular momentum

Conclusions :

- Accretion disk can be unstable in respect of Rossby waves, other types of instability
- An accreting magnetized star may be either in stable or unstable regimes
- Jets can be launched due to magnetic or centrifugal forces.